

ROAD FAILURES AND RELATED HAZARDS ALONG THE BLUE RIDGE
PARKWAY, NORTH CAROLINA

A thesis submitted to the faculty of
San Francisco State University
In partial fulfillment of
The requirements for
The degree

Master of Science
In
Applied Geosciences

by

Robert Joseph Sas, Jr.

San Francisco, California

May, 2008

Copyright by
Robert Joseph Sas, Jr.
2008

CERTIFICATION OF APPROVAL

I certify that I have read *Road failures and related hazards along the Blue Ridge Parkway, North Carolina* by Robert Joseph Sas, Jr., and that in my opinion this work meets the criteria for approving a thesis submitted in partial fulfillment of the requirements for the degree: Master of Science in Applied Geosciences: Geology at San Francisco State University.

Dr. Leonard Sklar
Assistant Professor of Geology

Dr. Jerry Davis
Professor of Geography

Dr. Mary Leech
Assistant Professor of Geology

Dr. L. Scott Eaton
Associate Professor of Geology
James Madison University

ROAD FAILURES AND RELATED HAZARDS ALONG THE BLUE RIDGE
PARKWAY, NORTH CAROLINA

Robert Joseph Sas, Jr.
San Francisco State University
2008

I studied the physical processes and impacts associated with failure of road-fills and downslope impacts, such as debris flows. I hypothesized that sites of arc-form pavement cracks signaled incipient road-fill failure and that the topography surrounding these sites could be used to extract a topographic signature of failed-or-cracked sites. I developed a method that uses virtual fieldwork to map pavement cracks, and verified in the field that this method is ~90% reliable. Using the methods of geographic information systems I was able to analyze slope distributions and develop a probabilistic hazard assessment model to predict such failures. Once the methods of analysis were defined, the model was automated using Python scripts and is poised for testing on roads other than the Blue Ridge Parkway. I tested the hazard assessment and road-closure protocols I developed, in a real-time simulation attended by federal and state land managers. The information gained from this workshop allowed me to make recommendations to land managers and policy-makers to improve hazard assessment by implementing an interagency cooperative.

I certify that the Abstract is a correct representation of the content of this thesis.

Chair, Thesis Committee

Date

ACKNOWLEDGEMENTS

I am greatly appreciative of and indebted to the numerous mentors, peers, friends, and family that have made this thesis possible, it is they who paved the road to my success. I thank Dr. L. Scott Eaton for his expert guidance, creativity, and mentorship that are largely responsible for the geologist I am today, and Dr. Leonard Sklar whose passion for quantification and thoughtful inquisitiveness continue to challenge my scientific and mathematic thinking. I thank Dr. Mary Leech for challenging me to see landscapes from the subsurface up, and for her lessons on grant-writing. I thank Dr. Jerry Davis for teaching me everything I know about Geographic Information Systems and for his help on Python scripts. I also thank Dr. Susan Russell-Robinson, Dr. Gerry Wieczorek, Thomas K. Collins, Paula Gori, J. David Anderson, Bambi Teague, John Dixon, Jim Amenta, Rick Wooten, Rebecca Latham, and Jackie Holt for advice and guidance throughout this work.

Table of Contents

List of Figures and Tables	viii
List of Appendices	x
1 Introduction.....	1
1.1 Project Scope	2
1.2 Regional Setting.....	6
1.3 History of the Blue Ridge Parkway	7
1.4 September 2004 road-fill failures on the Blue Ridge Parkway	10
1.5 Background	13
1.6 Project Design.....	14
2 Field Reconnaissance.....	16
2.1 Virtual Fieldwork.....	17
2.2 Field Methods and Observations	19
3 Probabilistic Hazard Evaluation Model	23
3.1 Data Sources and Analysis Buffer Calibration	24
3.2 Topographic Analysis and Slope Distributions	26
3.3 Statistical Analysis.....	28
3.4 RAMSLOPE – Geographic Information System Analysis Model	33
3.5 RAMSLOPE – Probabilistic Hazard Evaluation Model.....	34
3.6 Comparison to Existing Hazard Model – SHALSTAB.....	37
3.7 Model Limitations, Assumptions, and Experimental Error	39
4 Application for Management Practice	42
4.1 General recommendations to land managers	43
4.2 Prescribed use of hazard evaluation model.....	44
4.3 Road closure training and simulation workshop.....	45

4.4	Policy and planning considerations	47
5	Conclusions.....	51
6	Future Work.....	54
7	References.....	57
8	Figures and Tables	62

LIST OF FIGURES AND TABLES

Figure 1. Road-fill failure (a) and debris flow (b) at milepost 348.8, Blue Ridge Parkway. Photographs courtesy of Federal Highway Administration.....	63
Figure 2. Location map of study area showing locations of failed-or-cracked and a random selection of uncracked sites. Inset photo shows two debris flows initiated by road failures.	64
Figure 3. Rainfall from Hurricanes Frances and Ivan initiated numerous slope-failures in 2004. Modified from Neary and Swift, 1987.....	65
Figure 4. Distribution of landslide types initiated in September 2004. Used with permission (Collins, 2005).....	66
Figure 5. Photographs of road-fill failures and downslope impacts, shown by milepost (MP). Photographs courtesy of North Carolina Geological Survey and Federal Highway Administration.....	67
Figure 6. Schematic cross section of road-fill designs on Blue Ridge Parkway.	68
Figure 7. Screen capture of panoramic (160°) video and road inventory in VisiData.....	69
Figure 8. Automated road analyzer (ARAN) vehicle used to collect VisiData. Photo courtesy of Fugro-Roadware.....	70
Figure 9. Example of WiseCrax data output in VisiData.	71
Figure 10. Photograph of collapsed, undermined pavement indicating fill instability....	72
Figure 11. Biological and mineralogical evidence of prolonged, undesirable drainage condition of fill-slope (May 2007).....	73
Figure 12. Dripstone on retaining wall resulted from seepage through concrete-grout (May 2007).....	74
Figure 13. Terrain model showing topographic presence of Blue Ridge Parkway.	75
Figure 14. Irregular polygonal buffers generated in a GIS.....	76

Figure 15. Of three analysis buffers, the 30-m buffer was used for this study.....	77
Figure 16. The use of analysis buffers aided in the cell-by-cell extraction of slopes.....	78
Figure 17. Normalized-cumulative plot of pavement-removal from lumped, uncracked slope distributions.....	79
Figure 18. Normalized-cumulative plot of pavement-removal from lumped, failed-or-cracked slope distributions.....	80
Figure 19. Normalized-cumulative plot of lumped slope distributions.....	81
Figure 20. Frequency distributions of individual slopes.....	82
Figure 21. Probabilistic decision-making model.....	83
Figure 22. Flow chart of hazard assessment process using new methods.....	84
Figure 23. Under a false assumption, p-values were initially used to separate cracked and failed sites.....	85
Figure 24. Decision evaluation model.....	86
Figure 25. Plot of median slope vs. flow accumulation.....	87
Figure 26. Map comparing median slope GIS model output to SHALSTAB model.....	88
Figure 27. Student's t-test of SHALSTAB results.....	89
Table 1. Statistics from t-test for slope distributions.....	90

LIST OF APPENDICES

Appendix I: Index of Field Photos by Failed-or-Cracked Site	91
Appendix II: Modelbuilder diagram and Python scripts.....	104
Appendix III: Example of hazard evaluation exercise.....	116
Appendix IV: Data collected during virtual fieldwork	129
Appendix V: Road Closure Protocols.....	136

1 Introduction

1.1 Project Scope

Road-fill failures initiated during heavy rainfall are a common and serious management problem for transportation networks in mountainous terrain (e.g., Wemple et al., 2001; Larsen and Parks, 1997; Douglas, 1967). These failures can threaten human life, are costly to repair, and result in protracted road closures disrupting normal travel for months (Fig. 1). Fill failures can also result in debris flows (Collins, 2008), causing accelerated surface erosion and sedimentation in watersheds that can perturb the natural environment to the extent that some habitats are not recoverable (Furniss et al., 1991). Fill-type failures are an issue for all mountainous roads and are prevalent in aging roadways, especially those constructed in the 1930s and 1940s in National Parks and National Forests.

Commonly, these types of failures are mitigated or repaired once destabilization occurs, and little attention is given to predicting the location of future events over a larger region. Sediment yield from forested roads can be predicted using several analytical models (e.g., Elliot and Tysdal, 1999); however, few physically-based, analytical models that use site-specific field constraints are capable of predicting the initiation of failures themselves, especially on modified slopes. The main difference between the model I develop below and existing models is that the existing models are physically-based and calculate a factor of safety based on variables that are either held constant over the entire landscape (e.g., angle of internal friction, bulk density) (Dietrich et al., 1995) or have

limited site specificity (e.g., points to indicate landslide headscarsps) (Pack et al., 1998).

Other similar analyses have required intensive field investigations to collect data (Rollerson et al., 2002), whereas my methods require relatively little to no field work. The benefits of minimizing field work include a reduction in human resources and improved time-efficiency, both of which result in a reduction in monetary costs.

This study along the Blue Ridge Parkway (Fig. 2) was motivated by numerous landslides, occurring on modified and unmodified slopes, initiated by Hurricane Frances and Ivan in September 2004 (Collins, 2008; Wooten et al., 2008) (Fig. 3).

The erosional features associated with road failures during these rainfall events were particularly problematic because they occurred in cross-jurisdictional lands, a factor that often complicates landslide hazard zonation (van Western et al., 2006). On federally-managed lands, it is common for multiple agencies to be responsible for management of roads (Tom Collins, pers. comm.). The interagency cooperation that followed the storm impacts from the 2004 events motivated land managers to seek out a low-cost, time-efficient method for predicting similar future hazards. This need was recognized during a hazards workshop in November 2006, for which a preliminary “proof-of-concept” road failure map was used in a real-time hazards simulation.

Leading off of the concepts learned from the workshop, I developed a method that uses virtual fieldwork and a probabilistic model to quantify the topographic attributes associated with road-fill failure along the Blue Ridge Parkway in North Carolina

(Latham, 2006) (Fig. 2). Since topographic attributes have an increasing importance in understanding how natural landscapes function (e.g., Stock and Dietrich, 2006), it follows that these concepts be applied to modified landscapes, such as the failures under investigation. Slope angle is arguably the most fundamental of these attributes and is readily quantifiable from a digital elevation model (DEM). Field measurements can rarely capture topographic attributes at the scale and resolution necessary for a regional assessment of hillslope hazards (Dietrich and Montgomery, 1998). However, arc-shaped pavement cracks (hereafter referred to as “cracks”) observed in the field are a reliable indicator of gravity-driven failure of the fill material and has been used as a field constraint for fill-slope stability along the Blue Ridge Parkway (Collins, 2008).

With the aid of GIS tools and modeling, and by using a combination of virtual fieldwork using VisiData, field verification, and a high-resolution DEM, I was able to develop a model to provide a probabilistic hazard assessment of fill-slope stability along the Blue Ridge Parkway. “Virtual fieldwork” is defined as site-specific reconnaissance that yields accurate observations of on-site conditions and does not require on-foot or in the field investigation, and provides data at a higher-resolution and closer proximity than remote sensing data. This definition varies from the majority of published definitions in that I have implemented these methods purely for research purposes where most publications focus on educational uses of virtual fieldwork or virtual field trips (Stainfield et al., 2000).

Using a GIS, I was able to extract the most probable topographic signature of road-fill failure by determining the mean and variance of the slope distributions and flow accumulation [directly proportional to upslope contributing area] distributions adjacent to both cracked and previously failed sites. I also modeled Gaussian distributions from the statistical moments of the slope distributions and compared these to a random selection of road segments to develop a probabilistic decision-making model and a probabilistic decision-evaluation model for land managers. This probabilistic model can be used in forward or reverse and is therefore versatile for a variety of management and hazard assessment purposes.

I do not advocate my method or model as a replacement for on-foot evaluation of hazards nor as a complete model for assessing hazards. But rather, this method and modeling approach provide potentially useful, new tools that use existing datasets and technologies to minimize costs, and use a simple-conceptual approach accessible to land managers with little hazard evaluation experience. Land managers can use this hazard assessment to (1) focus field investigation efforts on susceptible areas; (2) mitigate potential impacts from susceptible slopes; (3) repair potentially unstable slopes; and (4) close susceptible portions of road during high-intensity rainfall.

1.2 Regional Setting

The Blue Ridge Parkway spans approximately 469 highway miles (~750 km) of rugged terrain in the Blue Ridge Physiographic province of the southern Appalachians, and links the Shenandoah National Park in Virginia with the Great Smoky Mountains National Park in North Carolina. The study area (Fig. 2) for this research is between milepost 310 at Linville Falls to milepost 370 near Craggy Gardens, northeast of Asheville, North Carolina.

The project sites lie within the Ashe Metamorphic Suite and Tallulah Falls Formation. The Ashe Metamorphic Suite consists of amphibolite schist and gneiss, pelitic schist and gneiss, and ultramafics. The Tallulah Falls Formation consists of metagraywacke, foliated to massive, interlayered and gradational with mica schist, muscovite-biotite gneiss, and rare graphitic schist (North Carolina Geological Survey, 1985; Merschat, 2006). Surficial soils are described as loose stone with some admixture of Porters loam (Federal Highway Administration, 2004).

The climate of Asheville (elevation 2,280 ft.) is humid temperate, with 47 inches of precipitation fairly evenly distributed throughout the year, and 15 inches of snow annually (National Climate Data Center, 2000); normal daily maximum temperatures for the past 30 years average 45.9° F in January and 83.3° F in July. Normal daily lows

average 25.3° F and 62.7° F for January and July, respectively. The higher elevations of Blue Ridge Parkway are lower in mean temperatures, and likely higher in precipitation.

In 2004, there were more hurricanes in the Atlantic basin than usual, with 15 named storms, six of which reached Category 3 on the Saffir-Simpson Hurricane Scale. Two of those storms impacted the southern end of the Blue Ridge Parkway between the dates of September 6–19, dropping as much as ~23 in. and ~10 in. of rainfall from Hurricanes Frances and Ivan, respectively (Beven, 2004). Despite Ivan ranking as one of the strongest Hurricanes on record (ninth most intense Atlantic hurricane on record, as well as the only Category 5 storm of 2004), Frances persisted for an extended period over the southern Appalachians, resulting in higher rainfall totals from that storm. The orography of the region has an important influence on weather systems and thus rainfall-initiated landslides (Wooten et al., 2008). Central within the study area is Mount Mitchell, the highest peak east of the Mississippi River at an elevation of 6,684 ft (Fig. 2).

1.3 History of the Blue Ridge Parkway

Development of the Blue Ridge Parkway was authorized by Congress under the National Recovery Act of 1933 and is contained in lands managed by the National Park Service, National Forest Service, and Federal Highway Administration. Construction

began on September 11, 1935 just south of the Virginia/North Carolina boundary, and the last section was paved in September 1987, although ~461 miles were completed by 1967. The section of road within the study area was built between 1938 and 1941 using construction methods from the original road building plan (Jackie Holt, pers. comm.). This type of construction required minimal excavation and fill-slopes were constructed from local micaceous soils. Testing of fill material collected from the September 2004 failures suggest that soils were not compacted to maximum density (Federal Highway Administration, 2004). Since modifications to the original construction plan occurred throughout the construction of the Blue Ridge Parkway, the condition of engineered fills may vary outside the study area.

The official purpose for construction was to provide a scenic-route connecting Shenandoah National Park in Virginia to Great Smokey Mountain National Park in North Carolina. The Parkway was built by laborers hired under the Civilian Conservation Corps and through the Works Progress Administration. Although President Herbert C. Hoover approved the National Recovery Act of 1933 and initiated construction of the adjoining Skyline Drive in Shenandoah National Park it was Franklin D. Roosevelt who approved final funding for the Blue Ridge Parkway late in 1933 (Jolley, 1969).

The Parkway was designed by landscape architect Stanley Abbott over the course of two years, authoring the original design documents including 800 pen-on-linen drawings. Numerous architects and engineers made modifications to these designs over

the nearly 50 years of original construction; however the goal of building a road that blended with the natural landscape was strictly maintained (Jolley, 1969; Roe, 2000). For this reason, the Blue Ridge Parkway can be considered a “sagging-rope road,” in which the road is considered analogous to a rope lowered across the landscape, coming to rest only under the force of gravity. Sagging-rope roads closely mimic the topography on which the road was constructed. This type of road construction is significant because it requires fewer cut-slopes and more fill-slopes.

Construction of the Blue Ridge Parkway is considered a significant accomplishment of landscape architecture and the many landscape architects who participated in its design and preservation were awarded the 2001 Classic Award by the American Society of Landscape Architects (American Society of Landscape Architects, 2001). The roadway travels through historically, culturally, and naturally important landscapes which warrants protection from slope-hazards.

1.4 September 2004 road-fill failures on the Blue Ridge Parkway

Although only four road-fill failures occurred in the study area during the September 2004 storms over 100 slope failures impacted National Forest lands surrounding the Blue Ridge Parkway (Fig. 4). Of these failures, road-fill failures were the most numerous; however the natural landslides that did occur constitute the most significant damages and impacts, including five human casualties (Wooten, 2008).

The four road-fill failures in the study area triggered by Hurricane Frances occurred along a six mile stretch from MP 345.3 to 351.1 (Fig. 5; Fig. 1), just southeast of the peak of Mount Mitchell (Latham, 2006). Two other fill-failures previous to 2004 were mapped in the field based on clear signs of reconstruction/mitigation (i.e., segment of newer pavement, rock gabions, and modern drainage structures); however no other specific information is available for these sites.

In general, all six failure sites occurred in engineered fill from the original Blue Ridge Parkway construction between 1938 and 1941 (Jackie Holt, pers. comm.). Borings from geotechnical studies prepared by the Federal Highway Administration revealed that the fill was constructed using a cut and cast technique comprised of sand, cobbles, and boulders of local origin (Federal Highway Administration, 2004). The fills ranged in depth from 4 to 20 feet in thickness. The large majority of the fill is derived from mica

schists that exhibit advanced stages of decomposition from chemical weathering. Standard penetration tests of the fill show compaction to be highly variable, and range from very loose to medium density (Federal Highway Administration, 2004). Similar tests of in situ bedrock show medium-to-very dense conditions. This variation in the fill density is likely due to the elastic nature of micas, making them difficult to compact once disaggregated, and can lead to eventual shifting and failing of engineered slopes.

The area around the failure at milepost 345.3 was initially repaired in 1997, where a 140 ft. section was reinforced using a geogrid system. This repair survived, but a proximal 210 ft. section of fill slope was damaged, impacting the northbound lane. The main scarp is arcuate in shape, suggesting a rotational component of slope failure. The scarp extends 10 ft. from the road shoulder, and exhibits a 6.5 ft. near-vertical face.

The failure around milepost 348.8 (Fig. 1) was a more substantial slope movement in that its eroded sediment entered a steep mountain tributary and traveled over a mile from its source (debris flow tracks shown in Fig. 2). The event likely started as a rotational slide on a planar fill-slope that translated to a debris flow (Fig. FS1). Although the volume of material originating from the fill was modest, the momentum carried by the mass allowed the continual accumulation of natural debris stored in the stream channels below, thus allowing the flow to travel nearly two miles. The failure also affected an adjacent overlook. The main scarp displays an arcuate pattern and extends a

full two feet into the southbound lane. The failure slope was steep, ranging from 45° to 67° (Federal Highway Administration, 2004).

The failure around milepost 349.1 was similar to that of milepost 348.8 in its style of movement and related debris-flow runout (see Fig. 2) within mountain tributaries. The fill-slope collapsed and translated into a debris flow that traveled an undetermined distance down slope. The main scarp is arcuate in shape, and extends 5 ft. from the roadway shoulder into the northbound lane. The headscarp showed 10–15 ft. of vertical drop, and the failure slope ranged from 45° to 90° (Federal Highway Administration, 2004). Paved waterway ditches leading to the site were noted, as well as an 18 in. corrugated metal pipe that once passed beneath the roadway.

The failure around milepost 351.1 was minor compared to the other three, as the section experienced only partial movement. The arcuate-shaped cracking was confined to 7 feet into the northbound lane, and crack openings were measured up to 2 in. of pavement rupture. Soils borings showed the presence of water and soft soils at grade with a culvert passing beneath the failure zone, suggesting the culvert may be compromised (Fig. 1). Additionally, I observed in the field that the culvert was plugged at its inlet and outlet, which can be an important factor contributing to fill-failure (Wemple et al., 2001).

1.5 Background

Multiple studies on the impact of land use and natural controls on road-related debris flows were carried out in humid–tropical (Douglas, 1967; Larsen and Parks, 1997) and monsoonal climates (DeGraff, 1990; Haigh et al., 1993). Although tropical storms are far more intense in these regions, rainfall totals are analogous to those observed in the Appalachian Mountains, and secondary controls are similar (Larsen and Parks, 1997; Sas and Eaton, 2008; Wooten, 2008). Few studies in the United States have focused on fill-slope failures (e.g., Wemple et al., 2001; Collins, 2008). Wemple et al. (2001) found that approximately two-thirds of sediment produced during an intense rainfall event in the Cascade Range of Oregon was produced from fill-slope failures. Fill-slope failures and other types of slope failures contribute sediment to mountainous drainages resulting in problems related to forest ecology, including salmon-habitat quality (e.g., Scott, 1982), increased surface runoff (e.g., Croke and Mockler, 2001), and forest harvest (e.g., Tague and Band, 2001). Field investigations of the failed portions of road and road-related debris flows showed that the failure surfaces were continuous between the road-fill and natural-failure slope (Latham, pers. comm.) (Fig. 1). This indicates that these debris flows initiate as road-fill failures that dilate and translate material through natural slopes.

The majority of studies relating road failures, landslides, and hazard susceptibility have employed bivariate and multivariate statistics (e.g., Larsen and Parks, 1997; Aleotti

and Chowdhury, 1999). While these methods are useful for demonstrating a statistical correlation between road failure and sediment yields, they cannot elucidate the triggering factors or feedback processes between natural and anthropogenically-related failures.

Dutton et al. (2005) used a numerical-modeling approach to simulate hydrologic effects of compacted forest-road surface on slope stability. However, this study modeled landslides originating upslope of the pavement surface as opposed to that of fill-slopes that are downslope of the pavement surface.

1.6 Project Design

The primary motivation for this project was the occurrence of numerous road-fill failures along the Blue Ridge Parkway in September 2004 (Collins, 2005). Following these intense rainfall events, federal land-managers recognized several needs for improved hazard assessment and mitigation of potential hazards including:

- (a) Process recognition of road-related slope hazards
- (b) A low-cost method for predicting road-fill failures
- (c) Development and testing of road-closure protocols
- (d) Development of an interagency-cooperative, hazard mitigation program

Each of these needs was addressed by my thesis work with significant progress in the development of a low-cost method for predicting road-fill failures. The main hypothesis of my research was, if topographic slope distributions capture the essential elements of slope stability and arc-shaped pavement cracks are a clear sign of incipient

failure, then the topographic attributes associated with locations of arc-shaped pavement cracks could be used to map potentially unstable locations along the road.

Field work was conducted to map previous and potential road-fill failures, and was also used to verify the results of the virtual fieldwork. I recognized several important factors contributing to road-fill failure along the Blue Ridge Parkway and collected several personal accounts from National Park Service employees regarding their observations prior to, during, and directly following road failure. The information collected through field observations, interviews, and from published articles provided a conceptual model to understand and recognize the factors and processes contributing to failure.

After an initial “proof-of-concept” hazard prediction model and road-closure protocols were developed, I co-led a workshop of federal-land managers to test the feasibility of real-time hazard assessment and subsequent closure of road segments determined to be hazardous. After successfully demonstrating the feasibility of such a hazard assessment and mitigation scenario, I worked with federal land managers and experienced hazards professionals to develop a preliminary interagency, hazards-mitigation program for the Blue Ridge Parkway in North Carolina.

2 Field Reconnaissance

2.1 Virtual Fieldwork

The initial reconnaissance of the pavement of Blue Ridge Parkway was fortunately made three months in advance of Hurricanes Frances and Ivan in the form of VisiData (Fig. 6). VisiData provides the virtual field environment and software interface to perform virtual fieldwork.

In June 2004, an instrumented truck traveling the full length of the Blue Ridge Parkway collected visual data of the viewscape, and the competency and conditions of the pavement. VisiData provides the user with a software interface for analyzing archived records of pavement conditions, including 160°-forward-view digital video, mosaic photographs of the pavement surface, observed drainage structures, and a spectral analysis of pavement surface conditions. All data were collected by three technicians operating a vehicle, called the automated road analyzer (ARAN) (Fig. 8), outfitted with various cameras, sensors and GPS. Much of this data collected by the ARAN was post-processed and checked for accuracy using automated algorithms and manually by technicians.

The spectral analysis is post-processed using bitmap pattern recognition techniques on images collected by WiseCrax (Fig. 9), a device composed of high-speed digital cameras and strobe lights on retractable booms. VisiData was developed by Fugro-Roadware for the Federal Highway Administration for its road inventory program. The

software and data were not initially intended for use in this type of slope stability analysis, but this research demonstrates that the VisiData is quite useful for this purpose.

The most significant resource provided by VisiData, for my purposes, was the seamless, digital video. The digital video captures travel lanes, drainage structures, and traffic safety controls, and provides excellent visualization of adjacent upslopes and good visualization of adjacent downslopes. In order to quantify the accuracy of the VisiData I investigated each highway mile in my 60-mile study area. Twenty-one sites of past or current pavement deterioration were documented during the field reconnaissance (Fig. 1), 19 of which were evident in the VisiData. Each site was identified via GPS coordinates, followed by a documentation of roadway conditions. There is a ~90% accuracy of virtual fieldwork given the ratio of accurate VisiData observations to accurate field observations. Data on the crack topology, dimensions, drainage structures, and other pavement conditions were recorded but have not yet been incorporated into the model due a limited dataset and lack of statistical correlation. VisiData is currently available for nearly all federally-managed, paved roadways including locations like Mount Rainier (James Amenta, pers. comm.), and is being implemented by numerous other agencies, both within the United States and internationally. Since VisiData has a variety of applications, the costs associated with data collection can be shared by various organizations that may benefit from its use. Additionally, VisiData could be a less expensive investment when

compared to on-foot fieldwork, especially for large study areas where it may not be possible to collect field data in a time-efficient manner.

The VisiData proved useful for virtual fieldwork to locate areas that showed evidence of cracking and progressive fill-failure. Although the video coverage included both travel lanes, the WiseCrax tool only analyzed the southbound lane, leaving the video as the only source of data for the northbound lane. Unfortunately, all four of the major failures in 2004 originated from the northbound lane, as much of the eastern slopes of the Blue Ridge Parkway are steeply dipping due to the Blue Ridge Escarpment and thus have with a strong influence on orographic precipitation and landslide initiation. However, in the most severe cases of road degradation, the pavement deterioration extended into both lanes, thereby registering with the WiseCrax tool. Overall, VisiData showed good agreement with field observations and as more VisiData is collected, I can establish a time series demonstrating the progressive nature of arc-shaped cracks.

2.2 Field Methods and Observations

The goals of my fieldwork were to collect data relevant to previous failures, map locations of arc-form pavement cracks, document the condition of drainage culverts, and evaluate the condition of repairs and mitigations. I collected data during two field outings, August 1–4, 2006 and May 28–29, 2007.

The 2006 field outing focused on studying previous failures and mapping the locations of pavement cracks. Three failures, located at mileposts 344.2, 348.8, and 349.1, were studied in detail. Fill material at milepost 344.2 did not experience a major failure from Hurricane Frances or Ivan, but did undergo partial reactivation during these rainfall events. The initial failure of milepost 344.2 constitutes the largest failure involving fill-slopes in the study area. This failure is of particular interest as a management problem because it involves lands managed by the National Park Service, Federal Highway Administration, United States Forest Service, and North Carolina Department of Transportation. The failure type was a rotational slump involving both lanes of the Blue Ridge Parkway, an onramp, and NC Rte. 80. Additionally, arc-form cracks were also reported to have been present prior to the failure occurring, as well as active seepage (or possibly dewatering) through the fill material just after failure (Alan Hollister, pers. comm.).

Degraded and failing culverts were observed in the field and were a contributing factor in road-fill failure (Fig. 10). One difficulty in observation was inability to see beyond the first few meters of pipe even with the aid of a high-powered flashlight. Nonetheless, locations of undermined and collapsed pavement often coincided with the orientation of culverts beneath the road surface.

Other evidence of fill-slope instability included biologic and mineralogic features associated with physical and hydrologic processes. The spatial distribution and mat

thickness of the moss growing on a retaining wall built to stabilize the toe of a fillslope provides evidence of the undesirable drainage condition of this fill-slope (Fig. 9). The moss detached from the wall due to flowing water, as evidenced by calcite mineralization. Linear discontinuities observed in moss growing on the wall face provided evidence that the concrete-grout that adheres individual rock cobbles together had degraded. As the minerals in the concrete-grout weather through time, the permeability increases leading to increased seepage. Additional observational evidence of seepage included small, dripstone and stalactitic structures of precipitating minerals, predominately calcite (Fig. 12).

The calcite mineralization process is complex considering the variable mineral content of shallow groundwater percolating through soil and in-situ rocks, in addition to minerals weathered from the concrete-grout and surrounding chlorite-mica schist cobbles in the wall. Went (1969) also suggests that this type of secondary-mineralization may have dependence on biological factors, such as fungal growth. Growth rates for calcium carbonate stalactites with similar formation conditions and issuing from similar materials, including concrete and limestone, range from ~0.02 to 1 in./yr. (Johnston, 1930; Ellis, 1931; Ver Steeg, 1932; Richards, 1932). A factor complicating comparison to these studies is the presence of vegetation and runoff to cause significantly different hydrologic conditions around the fill-slope compared to the hydrology of caves and bridges (Ver

Steeg, 1932). Given these rates of dripstone growth and the possible age of the wall (ca. 1937 to 1969), these processes likely began as early as ~1966 and as recently as ~2004.

3 Probabilistic Hazard Evaluation Model

3.1 Data Sources and Analysis Buffer Calibration

Model development and verification were performed in ArcMap 9.x, ArcView 3.x, and the final model was automated using Python scripts. Data from a GPS-delineated road polyline, a ~6-meter-resolution digital elevation model (DEM) (Fig. 13), VisiData, and field reconnaissance were used to develop a new approach to road-fill stability analysis. The road polyline was georeferenced in the field using VisiData. Light Detection and Ranging (LiDAR)-derived elevation data used in this study (available for download, North Carolina Department of Transportation, 2007) were collected in April 2007 after the 2004 landslides occurred. Although the National Park Service has jurisdiction over the Blue Ridge Parkway, the Federal Highway Administration is responsible for the majority of road maintenance and repair. The National Park Service is responsible for maintaining the historic and natural integrity of the landscape so the post-2004 repairs/mitigations were designed to mimic pre-2004 conditions. Since re-grading was done to the subsurface prior to installation of the post-2004 fill embankments with pre-failure surface morphology maintained, I considered the digital elevation data to represent the pre-2004 road-slope morphology and topology. However, it is impossible to replicate the exact pre-failure conditions so this is a potential source of error that cannot be accurately quantified without a pre-failure LiDAR DEM.

In order to analyze the slope distributions in a DEM, each grid cell containing a single value of elevation was extracted and included in a single distribution of slopes from within a calibrated, analysis mask. An analysis mask is any polygonal shape that delineates the boundary extents of any analysis of geographic information. Circular polygons were selected because other shapes or forms readily generated in a GIS are either irregularly shaped in general or the overlapping portions of individual polygons are irregularly bounded due to the sinuous nature of the roadway (Fig. 14). The circular polygons that served as analysis masks were generated from analysis buffers.

Several methods were used in an attempt to calibrate the most appropriate value for the radius of the analysis buffer. Initially, I generated a total of 3 buffer radii: 2,500 m., 90 m., and 30 m. (Fig. 15). The 2,500 m. buffer was selected based upon the maximum, runout distances of 2 road-related debris flows occurring in 2004 (~2,800 and 3,100 m., respectively). I chose the 90 m. buffer value somewhat arbitrarily, as it was the maximum distance of uninterrupted fill-material (e.g., no cut-slopes between fills) I measured in the field. The 30 m. buffer was logically determined based upon the dimensions of fill-embankment prisms measured in the field and using the high-resolution DEM. In general, the length (i.e., longitudinal distance along pavement) of road comprising fill extents was between ~45 and 75 m. as measured in the field. Typical widths (i.e., transverse distance from inbound pavement lane to downslope toe of fill) of fill extents were between ~30 and 60 m. measured from the DEM and estimated in the field.

Based upon these distances, a circular buffer with a radius of 30 m. was selected so that a 60 m. longitudinal segment of paved road could be analyzed at a time. In order to avoid potential analytical errors associated with an under-sized buffer, where actual fill-extents exceed the 30 m. radius buffer, I generated buffers from points located exactly 30 m from each other point. This ensured that each buffer would overlap ~40% of the area of each adjacent buffer so each buffer shared ~80% of its slope distribution with that of the adjacent two slope distributions. However, each value of median slope used in the hazard analysis is extracted independently, from within its own 30 m radius buffer where ~20% of its slope distribution is completely unique and is not shared with any adjacent buffers. Based upon this analysis I assumed that ~20% uniqueness and ~80% non-uniqueness of individual, slope distributions were sufficient to include fills outside the general range of dimensions and maintain some level of independence of the data between individual sites. The use of the 2,500 m. and 90 m. buffers was negated because they were simply too large in their spatial extents to provide meaningful site-specific evaluation.

3.2 Topographic Analysis and Slope Distributions

For my topographic analysis, I assume sites can be divided into two populations: unlikely to fail (stable) and likely to fail eventually (potentially unstable). Potentially unstable can be subdivided into those that previously failed, those that have arcuate

cracks and those that have not yet cracked or failed but are topographically similar to the cracked and failed sites. For purposes of the DEM analysis the failed and cracked sites are equivalent, because cracking was observed prior to failure at all but one of the six failed sites, and because I assume cracking indicates progressive failure which may lead to catastrophic road collapse as happened at the failed sites. Additionally, in developing the predictive model, I treat all uncracked portions of the roadway as part of the population of stable sites. After analyzing the distributions of the uncracked and failed-or-cracked sites, I discuss what fraction of the stable sites might actually belong to the potentially unstable population.

I extracted slopes from analysis buffers 30 m in diameter along the entire roadway (Fig. 16, total of ~130,000 grid cells). Included in this data set are cells occupied by the paved roadway, which has a nearly flat surface. To avoid skewing the slope distribution toward the low slope tail, I used a narrow buffer, 6 m in diameter to extract slopes from the paved roadway, and subtracted this distribution from the 30 m buffer data set (Fig. 17).

Several bridges and tunnels present in the study area were removed from this analysis since their engineered stability is unrelated to fill-slope stability and their presence in the DEM would unnecessarily skew the slope distributions. To characterize the slope distribution representative of the failed-or-cracked sites, I extracted slopes from 30 m radius circular buffers centered on the surveyed location of the cracks, for each of

the 21 failed-or-cracked sites (Appendix I). Each circular buffer contains ~70 cells. As illustrated in Figure 16, I used a 6 m radius buffer through each site to extract the slope values associated with the paved roadway (~18 cells per site), and then subtracted these values from the failed-or-cracked slope distributions for each site. Figure 18 shows the distributions of all slope values for all 21 sites combined, with and without the paved roadway data.

Finally, to fully separate the failed-or-cracked and uncracked slope distributions, I subtracted the lumped failed-or-cracked slope values from the entire roadway slope set, to obtain two distributions representative of the two distinct site populations, shown in Figure 19.

3.3 Statistical Analysis

I performed all statistical analyses using JMP 5.0.1. The failed-or-cracked and the uncracked road distributions were compared in normalized cumulative plots (Fig. 19) to draw general, quantifiable relationships among the data variables. Additionally, I employed Student's t-test (Student, 1908) to assess the significance of the difference between the means of the various distributions. Although the cracked-or-failed and uncracked distributions cover nearly the same range in slope values, they are distinctly different from one another. This is shown by a t-test comparing the mean slope for each

population, 31.6° for the failed-or-cracked sites and 21.9° for the uncracked portion of the roadway. The means are significantly different at a confidence level greater than 99.99% ($P > 0.9999$; statistics for t test are listed in Table 1).

My goal, however, is to identify potentially unstable sites that have not yet developed cracks. The basic question is, for a given site along the roadway, is the distribution of slopes within that site buffer more consistent with the failed-or-cracked slope distribution than the uncracked distribution? If so, then that site may have an elevated probability of developing cracks and progressive or sudden failure in the future. The lumped slope distributions shown on Figures 5 to 7 cannot be used directly for this; rather I must use the statistics for sets of individual sites.

I analyzed the slope distributions within each of the 21 individual failed-or-cracked sites and focused on the median slope within each site buffer as representative of the overall steepness of the site. The median is more robust against the slight skew of the slope distributions, whereas the mean is affected by this skew. I also randomly selected 21 sites from the uncracked portion of the roadway, and calculated the median slope from each slope distribution. The distributions of site-median slope for failed-or-cracked and uncracked sites are shown in Figure 20. Also shown are curves representing normal (Gaussian) probability density functions of site-median slope $p(S)$, given by

$$(1) \quad p(S) = \frac{1}{\sqrt{2\pi}\sigma} \exp\left(-\frac{(S-\mu)^2}{2\sigma^2}\right)$$

where μ and σ are the mean and standard deviation of the measured distributions respectively. Figure 20 indicates that the distribution of possible site-median slopes can be treated as normally distributed, as predicted by the central limit theorem.

Like the lumped slope distributions in Figure 19, there was a clear difference in the site-median slopes between the failed-or-cracked and uncracked portions of the roadway. I used the statistics of the site-median slope distributions to develop a model for evaluating the likelihood that any given currently uncracked site may be topographically more consistent with the failed-or-cracked sites than with the population of uncracked sites.

Figure 21 shows the cumulative distribution, $P_c(S)$, for the normal fit to the failed-or-cracked site-median slopes, given by

$$(2) \quad P(S) = \int_0^S p(s) ds$$

which describes the probability that any location which belongs to the population of potentially unstable sites will have a median slope less than or equal to S . Also plotted in

Figure 21 is the complementary cumulative distribution, $P_u^*(S) = 1 - P_u(S)$, which describes the probability that a site will have a median slope greater than or equal to S if it belongs to the stable, uncracked site population. Figure 21 shows that as site-median slope increases, the value of $P_u^*(S)$ declines, and the value of $P_c(S)$ increases, because steeper slopes are more likely to be unstable. Note that the two curves cross where the median slope equals $\sim 29^\circ$.

Probabilistically, any currently uncracked site could be considered more consistent with the stable uncracked distribution if the median slope S is less than 29° , and more consistent with the failed-or-cracked distribution for S greater than 29° . To quantify the odds (O_c) that a given site-median slope S is more appropriately considered to be part of the failed-or-cracked distribution, I use the expression

$$(3) \quad O_c = \frac{P_c(S)}{P_c(S) + P_u^*(S)}$$

where the sum $P_c(S) + P_u^*(S)$ encompasses all possible outcomes. Equation 3 states that O_c is the fraction of all outcomes represented by the probability that a site should be considered part of the cracked-or-failed distribution; O_c is thus constrained to vary between 0 and 1.

Prior to lumping the slope distributions from individual failed and cracked sites, I analyzed these distributions separately with the hypothesis that the highest mean slopes would likely be from locations that have previously failed. Of the 6 failed sites (Fig. 20), 5 have mean slopes that are at the lower tail of the distribution of failed-or-cracked sites ($n=21$). This result was not expected, as slope angle is a significant driving force for failure (according to the Mohr-Coulomb criterion), and therefore higher values of mean slope were expected to be associated with failure sites. This unexpected finding can be justified by a false assumption in how I initially classified the distributions of failed and cracked sites separately, when, in fact, they should be assumed to be from the same population. The importance of incorporating the two distributions into a single distribution is demonstrated by the fact that three of the four failures in 2004 showed arc-shaped cracks prior to complete failure of the fill material. These four failures occurred within a 10 km. segment of the Blue Ridge Parkway on the southwestern flank of Mt. Mitchell (elevation 6,684 ft. [~ 2040 m.]). Essentially, these basins received the greatest magnitude and intensity of rainfall from Hurricane Frances, nearly 24 in. (60 cm.) of total rainfall within a 24 hr. period, due to extreme orographic forcing. The observation that only one of these failures had not yet developed precursor signs of failure (i.e., arc-shaped cracks) strengthens my assumption that some sites that can potentially fail may not yet show precursor signals identifiable through virtual fieldwork or on-foot field

work. The transition of my focus from the false dichotomy of “failed” and “cracked” distributions negated the use of p-values (Fig. 23).

3.4 RAMSLOPE – Geographic Information System Analysis Model

The GIS methods applied to extract slope distributions and a method to analyze the statistical attributes was combined with the probabilistic hazard evaluation model to yield a combined model, called RAMSLOPE (Road Analysis of Median Slope and Landslide Occurrence Probabilistic Evaluation). The final GIS-based model used to analyze slope distributions and provide a map output was automated using Python scripts and a ArcGIS Modelbuilder model (coded by Jerry Davis and Barry Nickel, 2008, Appendix II). Python is a programming language that readily interfaces with ArcGIS and provides a means of easily distributing the model to end users, such as land managers. The model and scripts require some initial set-up, including defining the root folders for the input data files and destination folders for output file names. The buffer sizes can also be adjusted depending on the calibrated distance appropriate for the road under investigation.

The Modelbuilder model provides a visual approach to extracting and analyzing the slope distributions in combination with three Python scripts including Densify Arcs, Convert Line Vertices to Points, and Circle Statistics (Appendix II). The GIS model is also compiled into a single script that references the other three scripts (Compiled GIS Model Script, Appendix II). The GIS model first selects the segment of road and uses the

Densify Arcs script to break the road polyline into segments of a user-specified length (e.g., 30 m.). The Convert Line Vertices to Points script assigns a point feature to each vertex of the densified road line. The slope raster is then converted into a polygon shapefile and a series of buffers are used to extract by mask the slopes representing the paved surface. Circular buffers are applied to the road points and are used by the Circle Statistics script to analyze the slope distributions and calculate the statistical moments (e.g., mean, median, and standard deviation) and feature attributes (e.g., count of raster cells within each buffer) (Appendix II). The median can be symbolized in a variety of ways including proportionally sized circles and used to create a hazard map in conjunction with the probabilistic model.

3.5 RAMSLOPE – Probabilistic Hazard Evaluation Model

The probability-curve based, decision-making model gives land managers the ability to decide an acceptable level of confidence and relative false positives/negatives for determining the probability of road-fill hazards. For example, at an 80% level of confidence (G1 in Figs. 21 and 22), the hazard criterion differentiating the failed-or-cracked from the uncracked distributions is a median slope value of $\sim 33^\circ$. In a general sense, median slope values allocated to the left of line G2 (Fig. 21) are considered non-hazardous slopes and all to the right are considered hazardous.

Since probabilistic hazard assessment can never provide a useful decision with 100% confidence, there will always be some element of false negatives, where slopes are zoned as not hazardous when they truly are hazardous. Minimizing the probability of false negatives must therefore be balanced with the level of confidence. To evaluate the probability of false negatives it is useful to calculate the fraction of incorrect false negatives, or the rate of true positive (H1, Fig. 24). The rate of true positives for my example is ~0.14.

This rate suggests that ~14% of the slopes determined to be non-hazardous (less than value of G2) could be reclassified as hazardous. The improved uncertainty provided by the rate of true positives gives land managers several methods to further their hazard evaluation including (1) using the rate as the ideal percentage of road segments to study in the field and to randomly analyze in a GIS or with virtual fieldwork; (2) as a guide for establishing several levels of rates in an attempt to zone multiple, probabilistic levels of hazard; (3) to provide the public with a scientific basis for road closure during heavy rains; and (4) to determine whether other tools or datasets (e.g., flow accumulation) would further benefit the hazard assessment. Depending on the needs of the land manager and the goal of hazard assessment this decision making and decision evaluation model process can be done in reverse, where the first step is to determine the acceptable rate of true positives (Figs. 21, 22, 24).

There is a trade-off between higher levels of confidence and the rate of true positives. A higher level of confidence relates to higher values of median slope which deviate more from the mean of the normal distribution. This results in a decrease in the rate of true positives and a relative increase in the rate of false negatives. The decision ultimately comes down to the absolute acceptable error desired by the land manager or required by regulation. A minimum of >28% confidence is required because this is the point where the median slope has a 50-50 chance of being associated with either the failed-or-cracked or uncracked distributions.

In the event the land manager desires additional datasets to further their hazard analysis, I recommend using flow accumulation (Fig. 25). The means of the lumped, flow accumulation distributions for failed-or-cracked and random, uncracked sites were not statistically different from each other at an acceptable level of confidence. However, exponential trend lines fitted to the median slope and flow accumulation data is useful for parsing increased susceptibility for failure at the highest value of flow accumulation. Points falling closer to the trend line for failed-or-cracked sites may be considered part of the rate of true positives population and therefore used to better zone potentially hazardous sites.

3.6 Comparison to Existing Hazard Model – SHALSTAB

The use of slope and flow accumulation for GIS-based, landslide hazard assessment is not a new concept and is the premise of the physically-based shallow, landslide susceptibility model, Shallow Slope Stability model, or SHALSTAB (Dietrich et al., 1995). I compared my results with that of SHALSTAB and found that there was not a statistically significant relationship between the mean values of SHALSTAB susceptibility index at failed-or-cracked sites compared to uncracked sites (Fig. 27). The circles in Figure 27 are a graphical representation of the t-statistic, where the circles must overlap less than 5% of their area for the respective means to be significantly different. A likely reason why this physical-model may not show statistical agreement with mine is that it was not designed for assessment of modified slopes and is non-statistical in its approach to delineating hazards.

Although SHALSTAB is useful for a variety of purposes, the model assumes conditions for natural slopes and not modified slopes, whereas my model addresses modified slopes explicitly. SHALSTAB is more appropriate for users with a strong, physical understanding of slope stability who can expertly determine inputs for the model to function under its given assumptions, and not necessarily land managers *per se*. The probabilistic approach I offer is useful because it does not require iterative steps to calibrate the model nor expertise to assess hazards.

Furthermore, my approach uses some of the same physically-based assumptions regarding the ability of topography to describe some of the most important hillslope conditions relating to stability, but with an additional probabilistic hazard assessment. The application of virtual fieldwork to locate sites that show physical indications of instability also provides a physical basis for my model that I can treat statistically.

Figure 26 shows a portion of the roadway that was analyzed using my analytical model coded in Python script. The proportional symbols shown as circles represent ranges of median-slope classes. These symbols are shown over the output from the SHALSTAB model with the associated stability (susceptibility) index. The relationship between higher median slopes from my model and increasingly unstable slopes from SHALSTAB is apparent. However, much of the stability index surrounding the higher values of median slope along the road is closest to chronic instability with little variation between the SHALSTAB results. Since SHALSTAB zones the majority of these slopes as conditionally unstable to unconditionally unstable, the land manager would be left to determine discrete segments of roads as hazardous or not, either through intensive field work or their own hazard evaluation expertise.

3.7 Model Limitations, Assumptions, and Experimental Error

The presence of roads in a landscape changes the surface and subsurface hydrologic processes and can therefore influence hillslope process. The unnatural drainage patterns caused by roads can ultimately disturb the stability of the slope. Culverts were observed to be degraded and this could be another causal factor contributing to road-fill failure and arc-form pavement cracking. Reid and Dunne (1984) demonstrate that surface runoff and culvert drainage can initiate erosion of hillslopes and introduce sediment into lower elevations of the watershed. Montgomery (1994) further shows the control that drainage basin size and road network density have on landslide initiation. Although culverts are suspected to have had an influence on failure initiation based on field observations, my method and modeling approach does not account for such factors. Insufficient data are yet available as to the number, condition, location, and drainage capacity of culverts draining the Blue Ridge Parkway. This information would be sufficient to assess whether the current locations and drainage capacity are sufficient to drain the adjacent hillslopes and prevent undesirable drainage conditions. The condition of culverts is relevant because exfiltration of water from broken culverts into the fill-slope can more readily increase internal pore pressures than surface infiltration. This is a site-specific factor that would be difficult to model in a GIS, but could be investigated from a statistical approach, such as, a Monte Carlo simulation to predict the number and density of broken

culverts within a given area. Several proposals to implement a survey of culverts were informally discussed with land managers, however no program has to date been established.

In an attempt to better quantify the role of hydrology in the road failures, I analyzed flow accumulation, which showed less statistical correlation than the slope distributions. However, similar studies relating flow accumulation to landslide initiation have shown strong correlations between these variables (Dietrich et al, 1995). The key difference between these studies is that for my analysis I used circular buffers of a constant size, whereas Dietrich et al (1995) standardized flow accumulation over the basin area. A GIS model could also be developed to extract values of flow accumulation and basin area to calculate similar ratios, and could be incorporated into the RAMSLOPE model.

Another potential source of error comes with the assumption that arc-form pavement cracks are a sign of incipient failure of fill material. The presence of arc-form cracks in the pavement at the head escarpment of failures (Fig. 1; Fig. 6) strengthens this assumption, as do other signs of degradation of the fill (Fig. 10). However, arc-form pavement crack formation may not always be driven by processes directly related to road failure. Other factors could include: design-specified, differential settling of fill (i.e., compaction of fill *expected* by engineering specifications); a poorly constructed or maintained wearing surface; and impact loading. Attempts were made to minimize these potential sources of error by making thoughtful field observations. Careful consideration

and discussions with other geologists were conducted at each of the 21 sites included in my analysis. Based on observations from VisiData, a total of 61 sites were selected for field study (Appendix IV). Based on observations from VisiData, there were 19 sites showing past or present arcuate cracks. An additional two sites with arcuate cracks were observed in the field, for a total of 21 failed-or-cracked sites. According to field observations, ~24 of the 61 sites listed in Appendix IV were considered non-arc-shaped cracks and/or unrelated to fill-slope failure. This implies that the maximum rate (by simple division) of accurately observing the presence of arc-shaped pavement cracks with VisiData is ~90%. The rate of locations observed in VisiData that were determined by field observation to be dissociated from fill-slope failure is ~39%. This suggests an approximately 10 to 39% rate of disagreement between VisiData and field observations. The lower rate of disagreement is favored for this study because of the relative confidence in my field observations. Prior to looking at VisiData I had not observed arcuate cracks in the field, so this suggests that a VisiData user with more experience in observing arcuate cracks would have a higher rate of success. However, considerable variability of these rates on a road-to-road basis is likely, so these rates should be carefully assessed in future studies to confirm the intrinsic accuracy of VisiData in other regions.

4 Application for Management Practice

4.1 General recommendations to land managers

From an engineering perspective, increasing the factor of safety beyond 1.3, which is current federal standard for the Blue Ridge Parkway, would decrease failure susceptibility based on observations that previously repaired and mitigated sites have incurred reactivation (e.g., soil slumping and trees bending at top of toe-walls, newly formed arc-form cracks). WiseCrax (from VisiData) should be collected for both lanes, as this dataset was not entirely useful because many failures occur in the northbound lane and not in the southbound lane where WiseCrax data was collected. The Federal Highway Administration determined that VisiData collection in both lanes to be cost ineffective (James Amenta, pers. comm.), but this study provides information not available at the time this decision was made. Recent developments since the 2004 VisiData was collected suggest that Fugro-Roadware now has the capability of running the visual datasets in forward and reverse and could correct for VisiData runs in opposite directions and in only one lane (i.e., collect southbound lane in 2006, collect northbound lane 2 years later, and continue alternating thereafter). The cost of data collection could potentially be reduced by collecting complete VisiData in the southbound lane and only WiseCrax data in northbound lane.

4.2 Prescribed use of hazard evaluation model

The RAMSLOPE model is recommended for use by land-managers with the intended purpose of locating potentially unstable road-fill failure hazards explicitly. Few fill-slopes are built equally, but they share common characteristics (Fig. 1) as do the failures associated with rainfall initiation. RAMSLOPE is most appropriate for paved, sagging-rope type roads in mountainous topography. No a priori assumption regarding lithology was made during this analysis and thus is not necessary. However, it could be shown with further study that this model is sensitive to lithology, or other factors, and would therefore not be useful in all regions.

The potential for RAMSLOPE to have applicability on roads other than the Blue Ridge Parkway is strong given its few assumptions and probabilistic approach. Supposing that the topographic signature associated with failed-or-cracked sites on any road can be extracted at an acceptable level of statistical significance, then the Modelbuilder model and Python scripts can be applied to the road and hazards zoned. Probabilistic methods lend the model to exportability to other roads; however the odds of incorrectly or erroneously predicting a hazard is always present, but can be minimized with careful analysis of the available data. Sufficient data regarding the locations of previous failures and arc-form pavement cracks are needed for this analysis to be useful.

4.3 Road closure training and simulation workshop

I co-led a workshop with Dr. L. Scott Eaton¹, Paula Gori², Todd Grote³, Dr. Susan Russell-Robinson⁴ entitled *Landslide Workshop for Land and Resource Managers: Experimental Study on the Blue Ridge Parkway* on November 17, 2006, in Asheville, North Carolina. The conference was intended to open a dialogue with land managers and to test the feasibility of a hazard evaluation and road closure program on the Blue Ridge Parkway of North Carolina. A total of 23 interdisciplinary and interagency engineers, scientists, and land managers were assembled to represent the range of expertise available in government agencies. Workshop participants included landscape architects, civil engineers, engineering geologists, hillslope geomorphologists, hydrologists, hazards management specialists, law enforcement officers, road maintenance personnel, and park rangers, representing the National Park Service, United States Geological Survey, United States Forest Service, North Carolina Geological Survey, Federal Highway Administration, Army Corps of Engineers, and academia.

Introductory remarks explaining the purpose of the workshop and general principles of slope stability were followed by the latest field observations and testing of an early

¹ James Madison University, Harrisonburg, Virginia

² United States Geological Survey, Reston, Virginia

³ West Virginia University, Morgantown, West Virginia

⁴ United States Geological Survey, Reston, Virginia

road-failure hazard map of the study area for use with road closure protocols via the *Hurricane Lulu Scenario*. The workshop concluded with an open discussion of the usability of the hazard program and the effects of road-fill failures on public safety, regional economies, ecological health, and resource management. Participants identified key knowledge gaps and discussed preliminary recommendations for changing management practice.

The preliminary hazard map developed for the workshop was based almost entirely on field observations and hazards were delineated at a low resolution of one-mile intervals. The workshop leaders considered the lacking accuracy of the map as acceptable for its purpose as a means of testing the road-closure protocols. Nevertheless, the initial hazard map shows similarities with portions of the Blue Ridge Parkway later identified in this study to be particularly hazardous so there is a modicum of accuracy at minimum.

The *Hurricane Lulu Scenario* was a real-time simulation of the events and decision making that occurs during potentially hazardous rainstorms. Land managers were broken into groups and were given a set of worksheets containing maps (Appendix III), road closure protocols, and step-by-step instructions for assessing the hazards in a GIS. The GIS contained a state outline base map for North Carolina, topographic maps, a basic geologic map, road line, susceptibility zones, mileposts, points of previous failure locations, points of observed pavement cracks and their severity, hyperlinked photographs, and several DEM derived base maps. Participants used these map features

coupled with rainfall data to determine the temporal and spatial relationship between road failure hazards and precipitation to enact road closure.

Road-closure protocols (Appendix V) implemented during the scenario were given preliminary approval by the National Park Service as they were successful in facilitating communications between decision makers and those executing closures in the field. The two main factors limiting the success of road closure was the practice of removing road-closure gates at the end of winter for aesthetic reasons, and the lack of immediately available law enforcement personnel. The simplest solution could be to leave the closure gates *in situ* year round, as the Atlantic Hurricane season begins shortly after the seasonal transition into spring, and to seek additional support for law enforcement when forecasts anticipate heavy rains.

Participants discussed the experimental nature of the hazard program, its limitations and error potential, and the considerations for liability. Despite these caveats, the overall response of land managers was that the program presented during the workshop was extremely promising and needed relatively minor refinements once the final hazard maps were available for planning and management.

4.4 Policy and planning considerations

The most significant progress in hazard management produced from this conference was recognition that the cooperation of several agencies permits distribution of

management responsibilities, minimizes fiscal spending, and increases understanding of policy-based decision making using scientific information. Despite the use of easements in conservation practice (Roe, 2000), these findings highlight deficiencies in the current approach of federal hazard management in which state and local governments are mandated to independently perform research for review by federal officials (Schwab et al., 2005), whereas the approach of the workshop was to incorporate experts and stakeholders at all levels of government throughout the entire hazard evaluation and planning process.

The policy-driven approach could be supplemented by aligning management practices across all districts to mitigate hazards in a mutually beneficial manner. For instance, road-fill failures and related debris flows on the Blue Ridge Parkway affect lands administered by the National Park Service, Federal Highway Administration, Forest Service, the state of North Carolina, and the Commonwealth of Virginia. The policy-driven approach attempts to manage lands with federal policies that govern hazard evaluation done at the local level without sufficient policy support for hazards mitigation (Raymond, 2006). The interagency cooperative approach allows land managers to work between agencies and find common goals, such as maintaining the safety of the Blue Ridge Parkway, and compromising on competing directives, such as protecting the scenic and historic aspects of the landscape while protecting public safety. One proposed solution to the problem of road-fill failures was to remove all fills by cutting back all

slopes to bedrock. This solution was in conflict with the Park Service directive to maintain the scenic beauty of the Parkway, as the fill-slopes allow greater access to view the landscape compared to cut-slopes (J. David Anderson, pers. comm.).

Although the scale of the hazards are much greater than that of this study, the response to the widespread flooding caused by Hurricanes Katrina and Rita exemplify a breakdown of policy implementation and interagency cooperation (Raymond, 2006). The potential for prevention of failures is a significant opportunity presented by the interagency cooperative approach, whereas the policy-driven approach permits zonation of hazards and leaves only a single government entity to maintain the roadway (or levee), whose hazards have the potential to impact multiple jurisdictions. Mitigation strategies that can address the concerns of all jurisdictions in the path of potential slope-hazards could require only simple modifications to engineering designs, or to initiate and sustain communication between agencies throughout the hazards management process. Progress in this direction began in 2005 when the North Carolina Geological Survey implemented a study of federally, state, and locally managed lands to map existing hazards and model slope-failure susceptibility using the slope-stability model SINMAP, Stability Index Mapping (Pack et al., 1998). Their proposed methods address numerous issues of slope-stability throughout the study area and the highlands of North Carolina, but have not addressed a specific method to predict road-fill failures. My modeling and probabilistic

hazard zonation approach may help to supplement the work of the North Carolina Geological Survey.

5 Conclusions

The results of my research demonstrate that a variety of processes contributed to road-fill failure and that topography can be used to predict such failures with a given level of confidence. My field work shows that repaired fill-slopes may develop signs of incipient failure after mitigation occurs and could potentially undergo catastrophic failure. Other field observations indicated degraded culverts, retaining walls, and shallow surface slumping are likely related to failure, but mapping their extents in the field was much more challenging than mapping arc-form pavement cracks. The accuracy of virtual fieldwork to map arc-form pavement cracks suggests that this method could be used on other roads that already have VisiData available.

The RAMSLOPE model generated to predict failures based on the locations of arc-form pavement cracks provides a cost-effective hazard evaluation tool to land managers. Land managers can use this model to zone hazards along the roadway and to use its map outputs to assess the potential for downslope impacts. The probabilistic approach to hazard zonation lends itself to use in a variety of geographic and geologic settings, however this has not yet been fully evaluated. In general, the map outputs from SHALSTAB agreed with the map outputs from RAMSLOPE, but were not statistically useful for delineating hazards of discrete segments of the Blue Ridge Parkway.

I consider my research a product of interagency cooperation because it was initiated and funded by federal agencies, but outside of policy-driven associations. Implementation of this research can only highlight the usefulness of the interagency cooperative and

interdisciplinary approaches to land management. By conferring with federal land managers and scientists I elucidated the negative aspects of current policy and provided recommendations for decision- and policy-making. Several minor changes could greatly improve hazard management on the Blue Ridge Parkway, such as leaving road-closure gates up year-round and initiating interagency communications besides those required by policy.

6 Future Work

The results of this study could be supplemented and improved by testing RAMSLOPE in other locations using 10-m DEMs, modeling hydrologic conditions associated with road-fill failure, studying geometries of constructed fills and controls on groundwater seepage.

In general, several assumptions of this work should be evaluated by applying the RAMSLOPE modeling approach to roads other than the Blue Ridge Parkway. The accuracy of my virtual fieldwork approach compared to that of field observation begs an evaluation of the fundamental applicability of virtual fieldwork. I recommend that future workers continue to apply their knowledge and experience to evaluating road-fill failure hazards in the field and not rely completely on the virtual fieldwork approach until better validated. Furthermore, the availability of LiDAR elevation data is limited, but 10-m DEMs are available for most of the United States and much of the world. Assessing the useability of 10-m DEMs with these methods is of vital importance to their applicability outside the Blue Ridge Parkway.

Surveys of culverts draining fill-slopes would be useful for informing physical-hydrology models. There is insufficient data regarding the mechanisms for and types of culvert degradation, so a visual inspection using periscopic or fiberoptic technologies to view the physical condition within culverts would be helpful.

Although some modeling of fill-slopes is apparent in the literature, few are well-constrained physically and all lack versatility. Better modeling of hydrologic conditions

associated with road-fill failure, especially with reference to geometric boundary conditions, degraded culvert seepage, and infiltration into pavement cracks, would significantly improve the current understanding of the physical processes involved. Improved physical-hydrology models are also important for recognizing conditions occurring at the scale of field observation and needs to be done in order to better parameterize analytical and probabilistic models, as well as informing the factor-of-safety based approaches to fill-slope design. Of direct importance to my research is deepening the knowledge base of how modified slopes interact hydrogeomorphically with natural topography, and this could be accomplished through hydrologic modeling.

7 References

- Aleotti, P., and Chowdhury, R., 1999, Landslide hazard assessment: summary review and new perspectives. *Bulletin of Engineering Geology and Environment*, v. 58, p. 21–44.
- American Society of Landscape Architects, 2001, The places we love to use: 2001 professional awards announcement (press release). Online resource:
<http://www.asla.org/nonmembers/publicrelations/pressreleases/pressawds092201.htm>
- Beven II, J.L., 2004, Tropical cyclone report hurricane Frances. National Weather Service National Hurricane Center. Online resource:
<http://www.hpc.ncep.noaa.gov/tropical/rain/frances2004filledrainblk.gif>
- Collins, T.K., 2008, Debris flows caused by failure of fill slopes: early detection, warning, and loss prevention. *Landslides*, v. 5, p. 107–120.
- Collins, T.K., 2005, Preliminary Assessment of Landslides Triggered by September 2004 Hurricanes Frances and Ivan on the Nantahala and Pisgah National Forests. United States Forest Service, 23 p.
- Croke, J., and S. Mockler, 2001, Gully initiation and road-to-stream linkage in a forested catchment, southeastern Australia: *Earth Surface Processes and Landforms*, v. 26, p. 205–217.
- DeGraff, J.V., 1990, Landslide dams from the November 1988 storm event in southern Thailand: *Landslide News*, Japan Landslide Society, v. 4, p. 12–15.
- Dietrich, W.E., R. Reiss, M.L. Hsu, and D.R. Montgomery, 1995, A process-based model for colluvial soil depth and shallow landsliding using digital elevation data: *Hydrological Processes*, v. 9, p. 383–400.
- Dietrich, W. E., and D. R. Montgomery, 1998, Hillslopes, channels and landscape scale; In G. Sposito (eds) *Scale Dependence and Scale Invariance in Hydrology*, Cambridge University Press, p. 30–60.
- Douglas, I., 1967, Natural and man made erosion in the humid tropics of Australia, Malaysia, and Singapore: International Association of Scientific Hydrology, v. 75, p. 17–30.

- Dutton, A.L., K. Loague, and B.C. Wemple, 2005, Simulated effect of a forest road on near-surface hydrologic response and slope stability. *Earth Surface Processes and Landforms*, v. 30, p. 325–338.
- Elliot, W.J., and S.A. Lewis, 2000, Linking the WEPP Model to Stability Models: Proceedings of the ASAE Annual International Meeting, paper no. 002150
- Elliot, W.J., and L.M. Tysdal, 1999, Understanding and reducing erosion from insloping roads. *Journal of Forestry*, v. 97(8): 30–34
- Ellis, R.W., 1931, Concerning the rate of formation of stalactites. *Science*, v. 73, p. 67–68
- Federal Highway Administration, 2004, Emergency landslide repair Blue Ridge Parkway, McDowell and Yancey County, North Carolina, Geotechnical Report No. 17-04, p. 1–11.
- Furniss, M.J., T.D. Roelofs, and C.S. Yee, Road construction and maintenance, *in* Meehan, W.R. (ed.), Influences of forest and rangeland management on salmonid fishes and their habitats: American Fisheries Society Special Publication 19, p. 297–324.
- Haigh, M.J., J.S. Rawat, S.K. Bartarya, and M.S. Rawat, 1993, Factors affecting landslide morphology along new highways in the central Himalaya—preliminary results: *Catena*, v. 15, p. 539–553
- Johnston Jr., W.D., 1930, The rate of growth of stalactites. *Science*, v. 72, p. 298–299
- Jolley, H.E., 1969, The blue ridge parkway. University of Tennessee Press: Knoxville, 172 p.
- Larsen, M.C. and J.E. Parks, 1997, How wide is a road? The association of roads and mass-wasting in a forested montane environment. *Earth Surface Processes and Landforms*, v. 22, p. 835–848.
- Latham, R.C., 2006, Slope stability along the North Carolina section of the Blue Ridge Parkway. *Geological Society of America Abstracts with Programs*, v. 38, p. 28.
- Montgomery, D. R., 1994, Road surface drainage, channel initiation, and slope instability. *Water Resources Research*, v. 30, p. 1925–1932.

- Merschat, C.E., B.L. Cattanach, M.W. Carter, and L.S. Wiener, 2006, Geology of the Mesoproterozoic basement and younger cover rocks in the west half of the Asheville 100,000 quadrangle, North Carolina and Tennessee; an updated look, *in* Labotka, T.C., Hatcher, R.D., Jr., eds., Geological Society of America, 2006 Southeastern Section Meeting: Field Trip Guidebook, p. 1–56.
- National Climate Data Center, 2000, Asheville North Carolina Monthly Normals. Online resource: <http://cirrus.dnr.state.sc.us/cgi-bin/sercc/cliMAIN.pl?nc0301>
- Neary, D.G. and L.W. Swift, Jr., 1987, Rainfall thresholds for triggering a debris avalanching event in the southern Appalachian Mountains: Reviews in Engineering Geology, v. 7, p. 81–92.
- North Carolina Geological Survey, 1985, Geologic map of North Carolina. North Carolina Geological Survey: Raleigh
- Pack, R. T., D. G. Tarboton and C. N. Goodwin, 1998, The SINMAP Approach to Terrain Stability Mapping. Paper Submitted to 8th Congress of the International Association of Engineering Geology, Vancouver, British Columbia, Canada 21-25 September 1998.
- Raymond, J.B., 2006, Hurricane Katrina and the paradoxes of government disaster policy: bringing about wise governmental decisions for hazardous areas. *The Annals of the American Academy of Political and Social Science*, v. 604, no. 1, p. 171-191
- Reid, L.M. and T. Dunne, 1984, Sediment production from forest road surfaces. *Water Resources Research*, v. 20, p. 1753–1761.
- Roe, C.E., 2000, Use of conservation easements to protect the scenic and natural character of the Blue Ridge Parkway: a case study. *In:* Gustanski, J.A. and Squires, R.H. (eds), Protecting the land: conservation easements past, present, and future. Island Press: Washington, D.C., 566 p.
- Richards, G., 1932, The growth of stalactites. *Science*, v. 75, p. 50
- Sas, R.J. Jr., and L. S. Eaton, 2008, Geologic controls on debris flow initiation and rates of basin denudation in the central Appalachian. *Landslides*, v. 5(1), p. 97-106.

- Schwab, J.C., P.L. Gori, and S. Jeer (eds), 2005, Landslide Hazards and Planning. American Planning Association, Report No. 533/534, 208 p.
- Scott, K.M., 1982, Erosion and sedimentation in the Kenai River, Alaska: U. S. Geological Survey Professional Paper, 39 p.
- Stainfield, J., P. Fisher, B. Ford, and M. Solem, 2000, International virtual field trips: A new direction? *Journal of Geography in Higher Education*. v. 24, p. 255–262.
- Stock J.D. and W.E. Dietrich, 2006, Erosion of steepland valleys by debris flows. *Geological Society of America Bulletin* v. 118, p. 1125–1148
- Student, 1908, The probable error of a mean. *Biometrika*, v. 9, p. 1–25.
- Tague, C. and L. Band, 2001, Simulating the impact of road construction and forest harvesting on hydrologic response, v. 26, p. 135–151.
- van Westen, C.J., T.W.J. van Asch, and R. Soeters, 2006, Landslide hazard and risk zonation—why is it still so difficult?. *Bulletin of Engineering Geology and Environment*, v. 65, p. 167–184.
- Ver Steeg, K., 1932, Stalactites and stalagmites growing above ground. *Science*, v. 75, p. 217
- Wemple, B.C., F.J. Swanson, and J.A. Jones, 2001, Forest roads and geomorphic process interactions, Cascade Range, Oregon. *Earth Surface Processes and Landforms*, v. 26, p. 191–204.
- Went, F.W., 1969, Fungi associated with stalactite growth. *Science*, v. 166, p. 385–386
- Wooten, R.M., K.A. Gillon, A.C. Witt, R.S. Latham, T.J. Douglas, J.B. Bauer, S.J. Fuemmeler, and L.G. Lee, 2008, Geologic, geomorphic, and meteorological aspects of debris flows triggered by Hurricanes Frances and Ivan during September 2004 in the Southern Appalachian Mountains of Macon County, North Carolina (southeastern USA). *Landslides*, v. 5, p. 31–44.

8 Figures and Tables



Figure 1. Road-fill failure (a) and debris flow (b) at milepost 348.8, Blue Ridge Parkway.
Photographs courtesy of Federal Highway Administration.

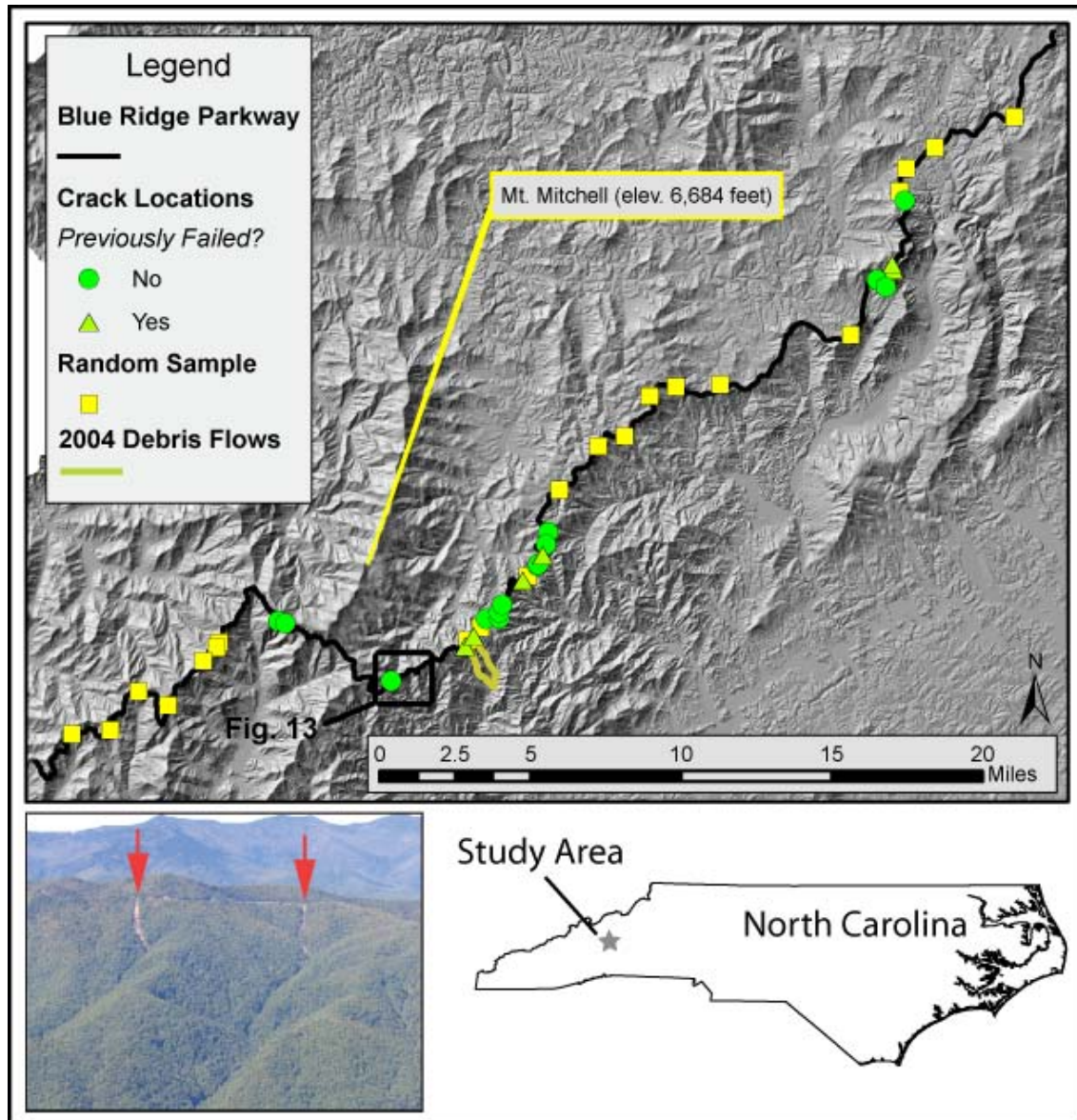


Figure 2. Location map of study area showing locations of failed-or-cracked and a random selection of uncracked sites. Inset photo shows two debris flows initiated by road failures.

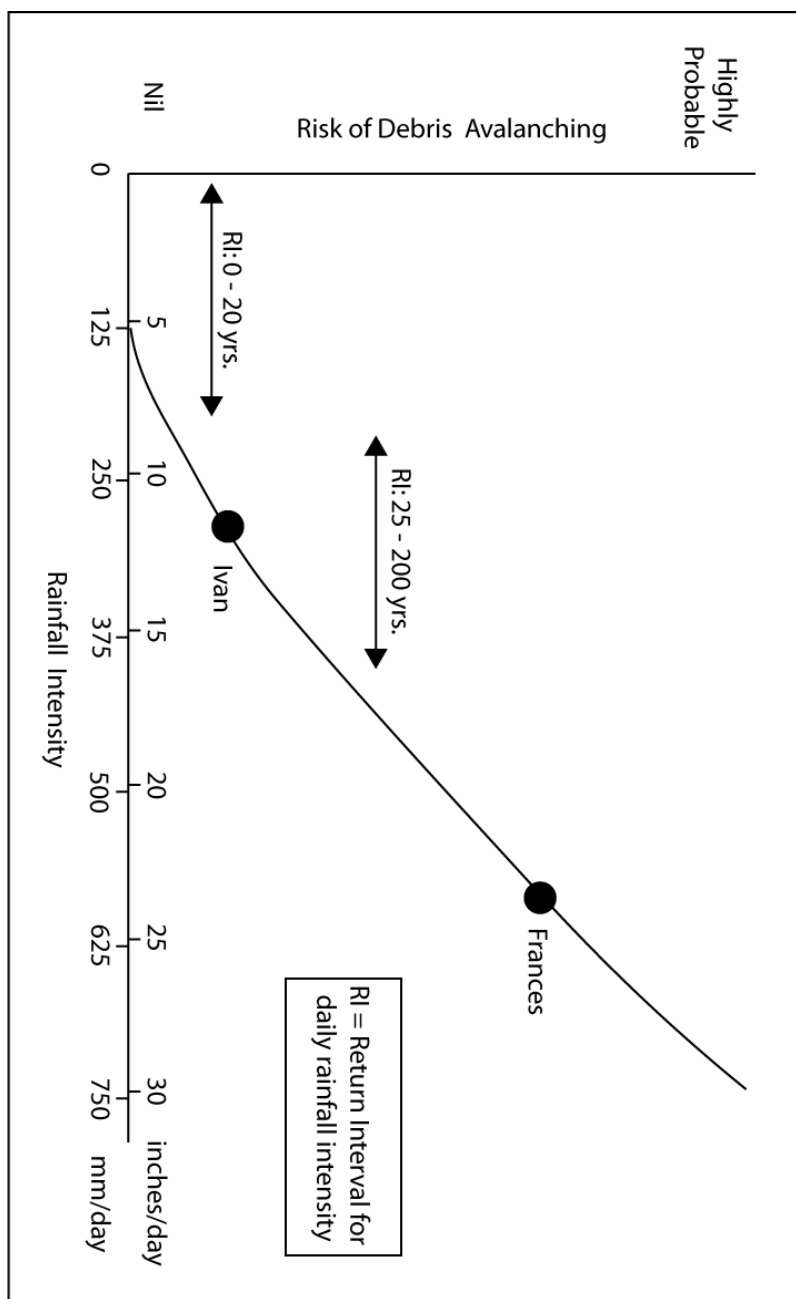


Figure 3. Rainfall from Hurricanes Frances and Ivan initiated numerous slope-failures in 2004. Modified from Neary and Swift, 1987.

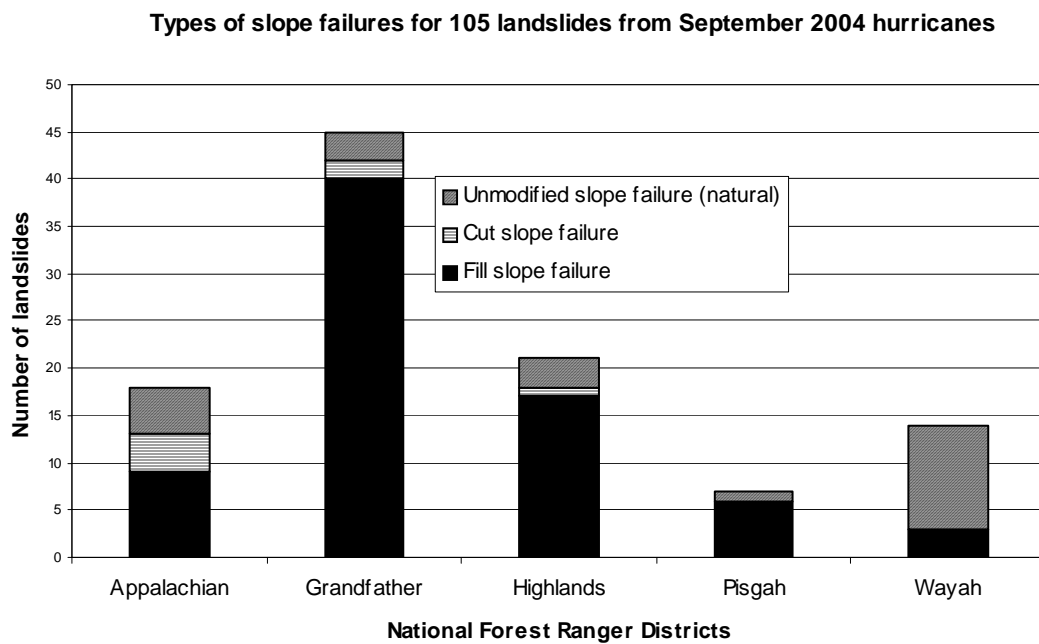


Figure 4. Distribution of landslide types initiated in September 2004. Used with permission (Collins, 2005)



Figure 5. Photographs of road-fill failures and downslope impacts, shown by milepost (MP). Photographs courtesy of North Carolina Geological Survey and Federal Highway Administration.

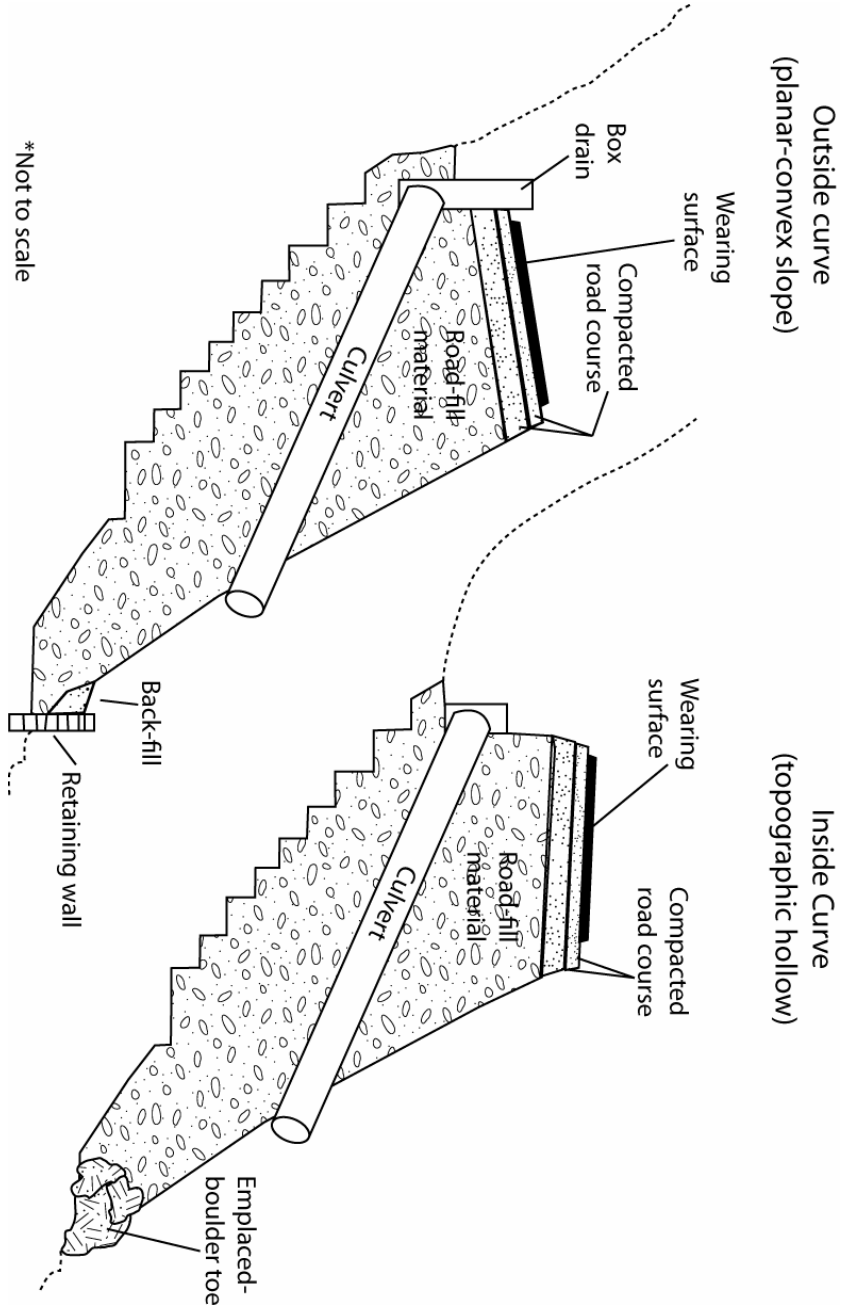


Figure 6. Schematic cross section of road-fill designs on Blue Ridge Parkway.



Figure 7. Screen capture of panoramic (160°) video and road inventory in VisiData.



Figure 8. Automated road analyzer (ARAN) vehicle used to collect VisiData. Photo courtesy of Fugro-Roadware.

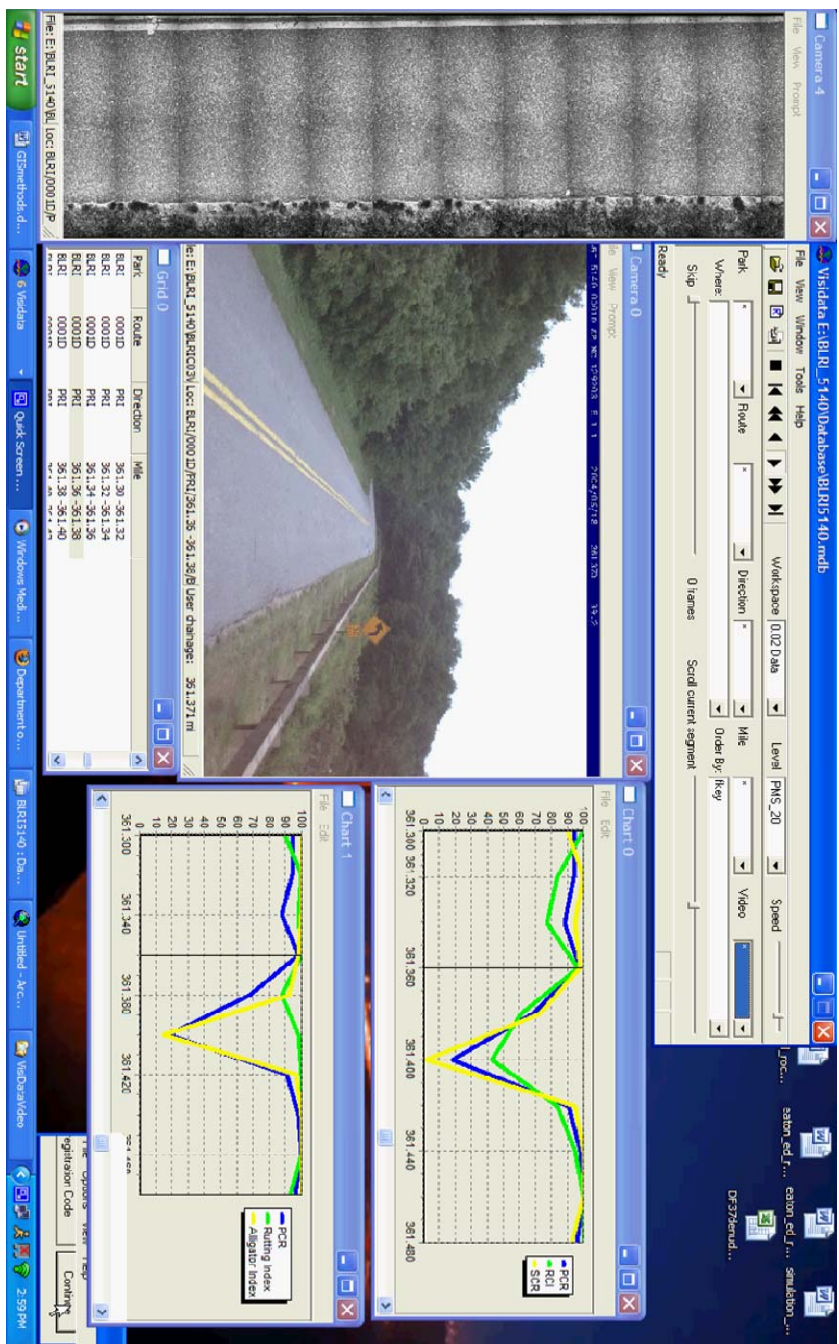


Figure 9. Example of WiseCrax data output in VisiData.



Figure 10. Photograph of collapsed, undermined pavement indicating fill instability.



Figure 11. Biological and mineralogical evidence of prolonged, undesirable drainage condition of fill-slope (May 2007).



Figure 12. Dripstone on retaining wall resulted from seepage through concrete-grout (May 2007).

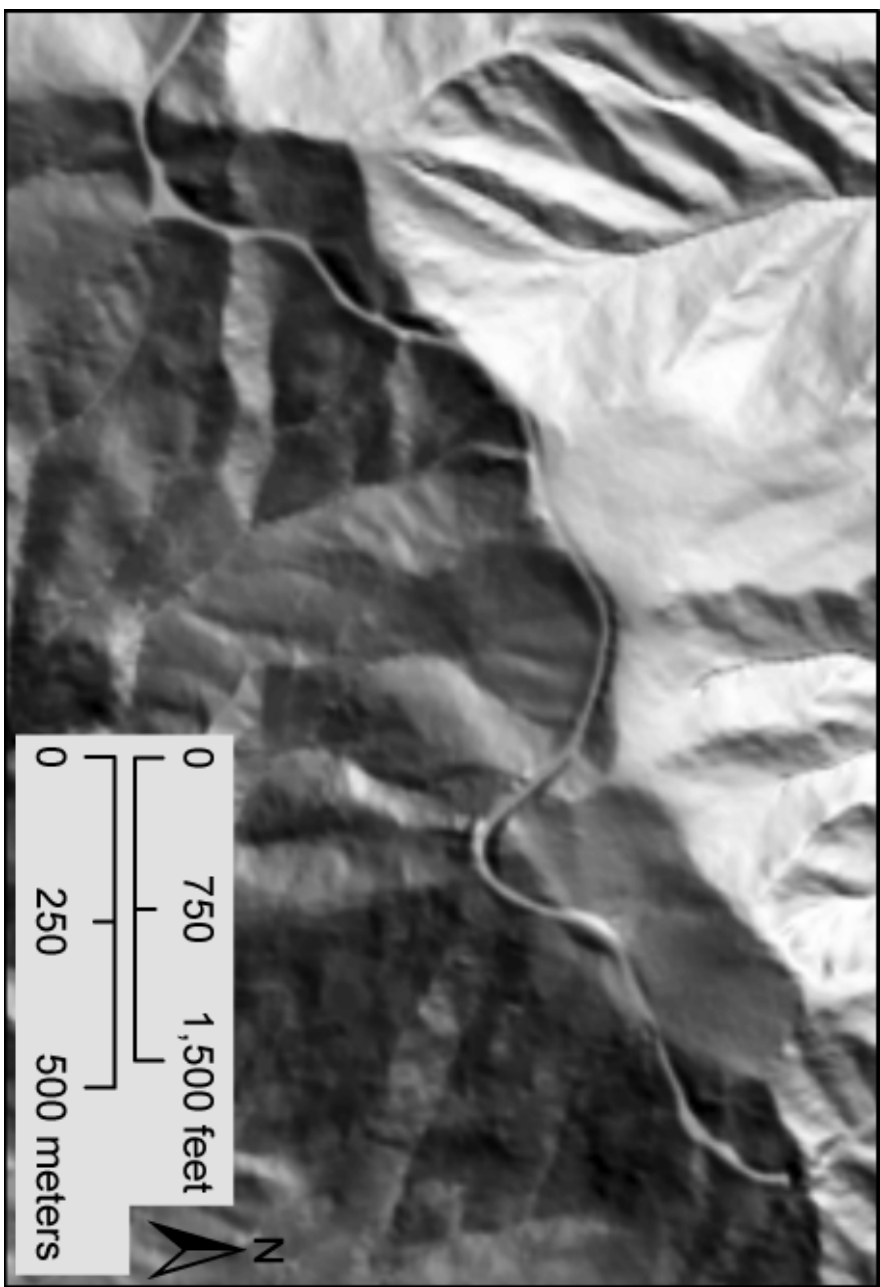


Figure 13. Terrain model showing topographic presence of Blue Ridge Parkway.

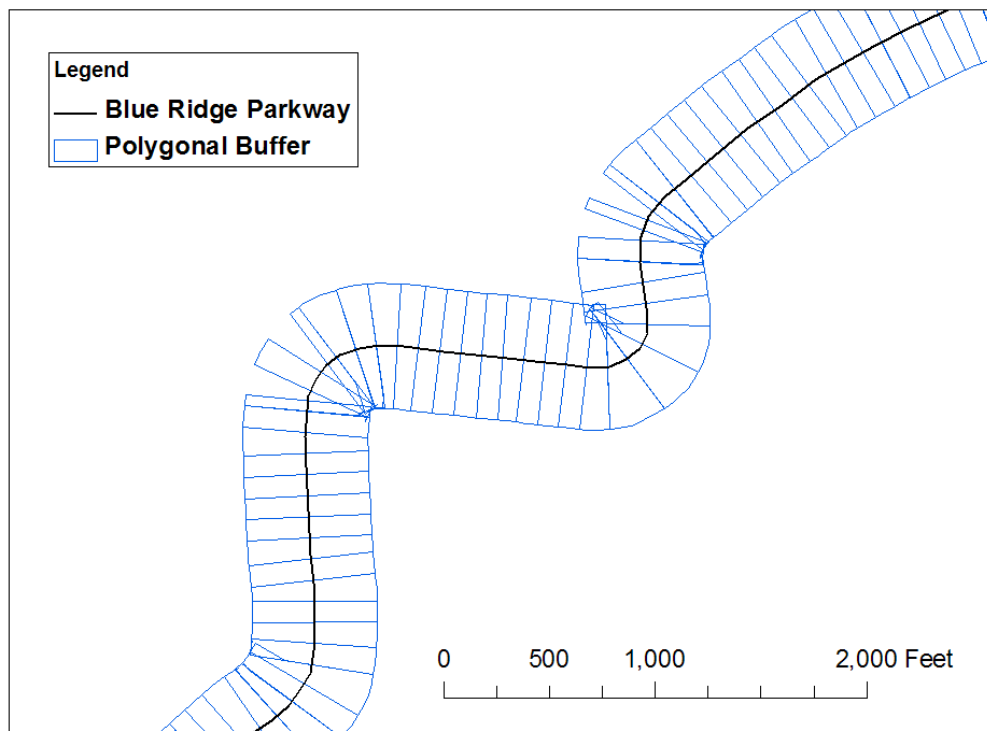


Figure 14. Irregular polygonal buffers generated in a GIS.

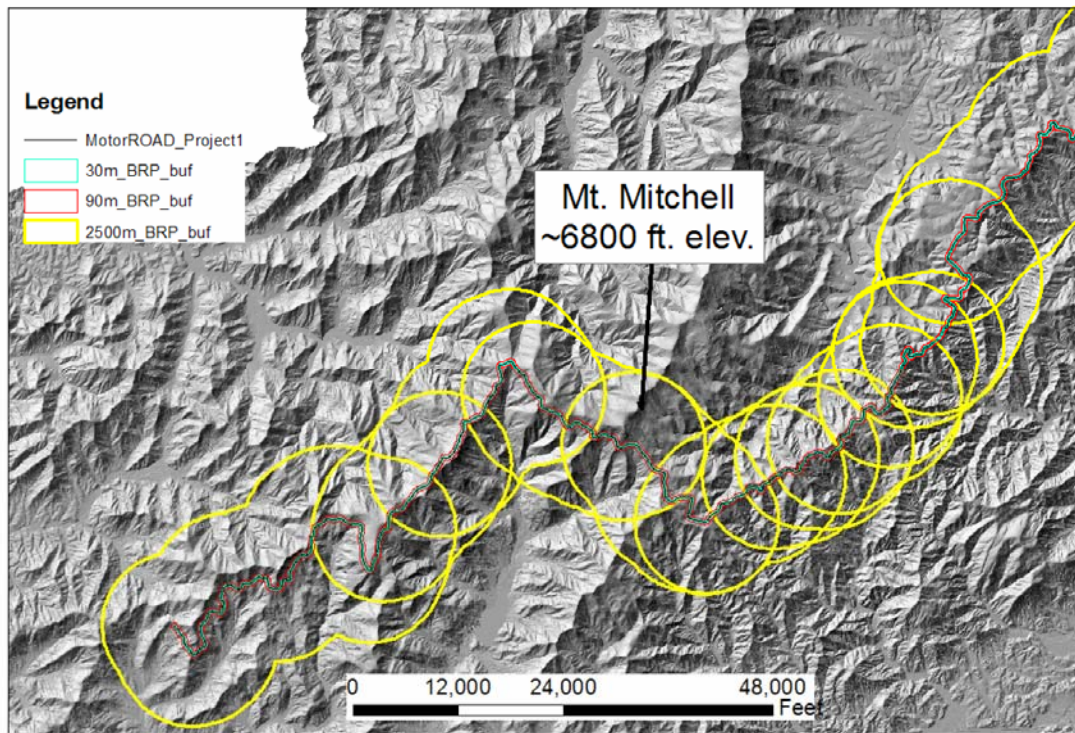


Figure 15. Of three analysis buffers, the 30-m buffer was used for this study.

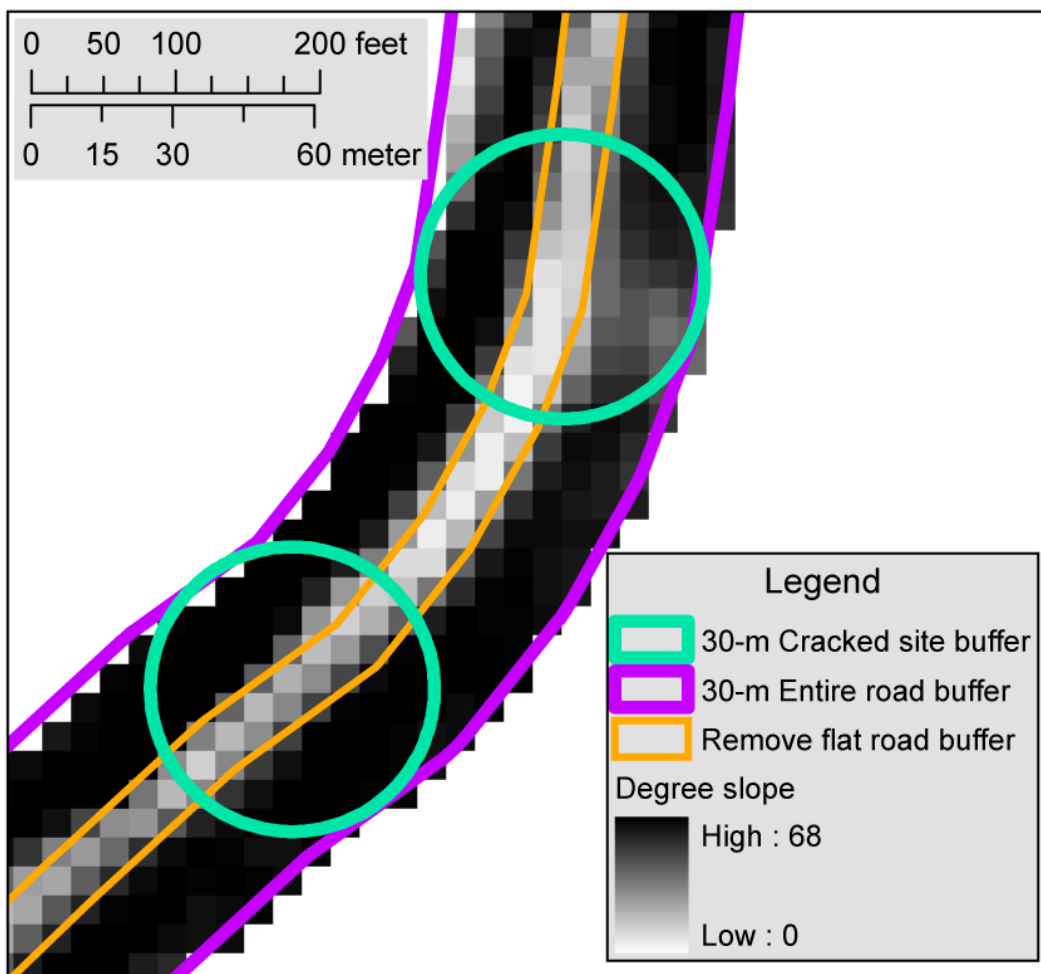


Figure 16. The use of analysis buffers aided in the cell-by-cell extraction of slopes.

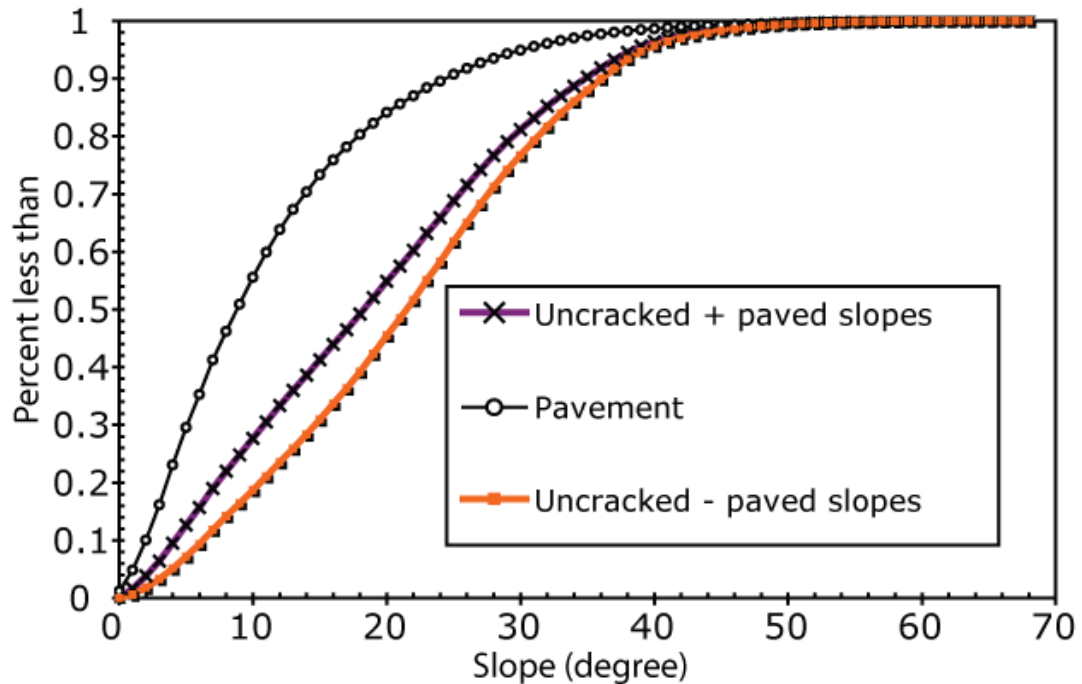


Figure 17. Normalized-cumulative plot of pavement-removal from lumped, uncracked slope distributions.

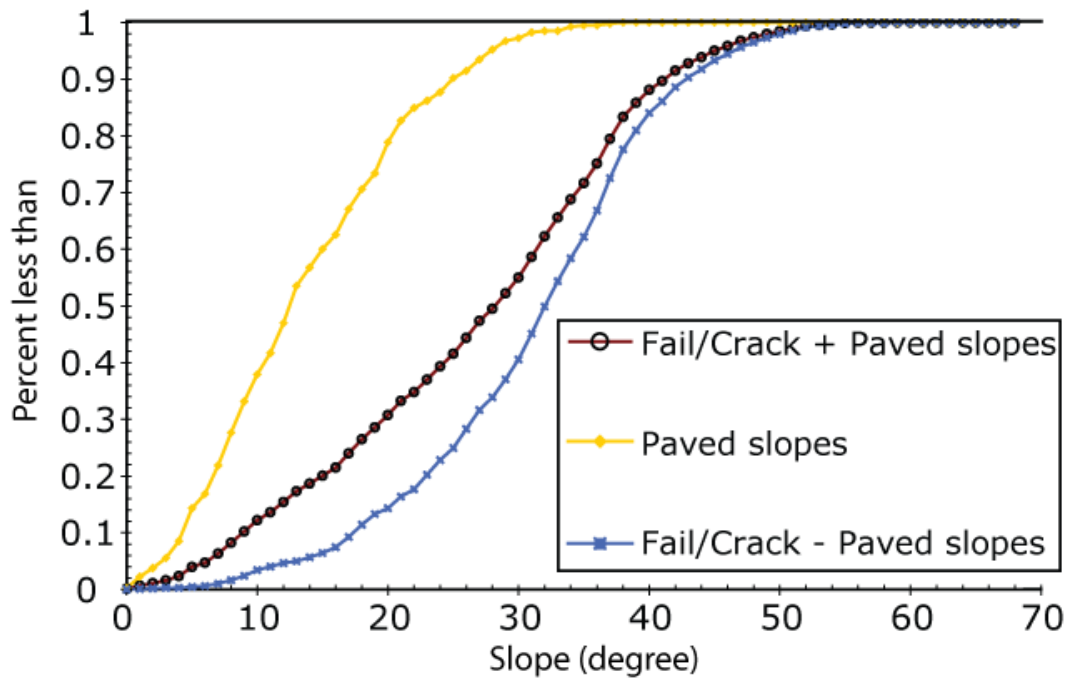


Figure 18. Normalized-cumulative plot of pavement-removal from lumped, failed-or-cracked slope distributions.

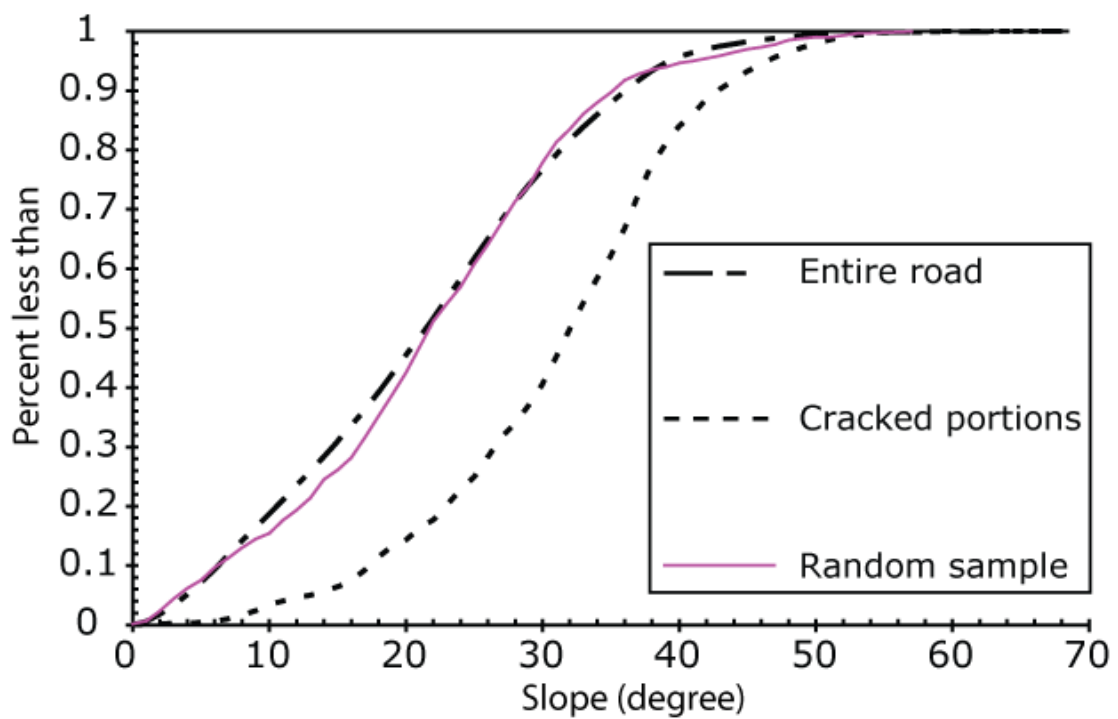


Figure 19. Normalized-cumulative plot of lumped slope distributions.

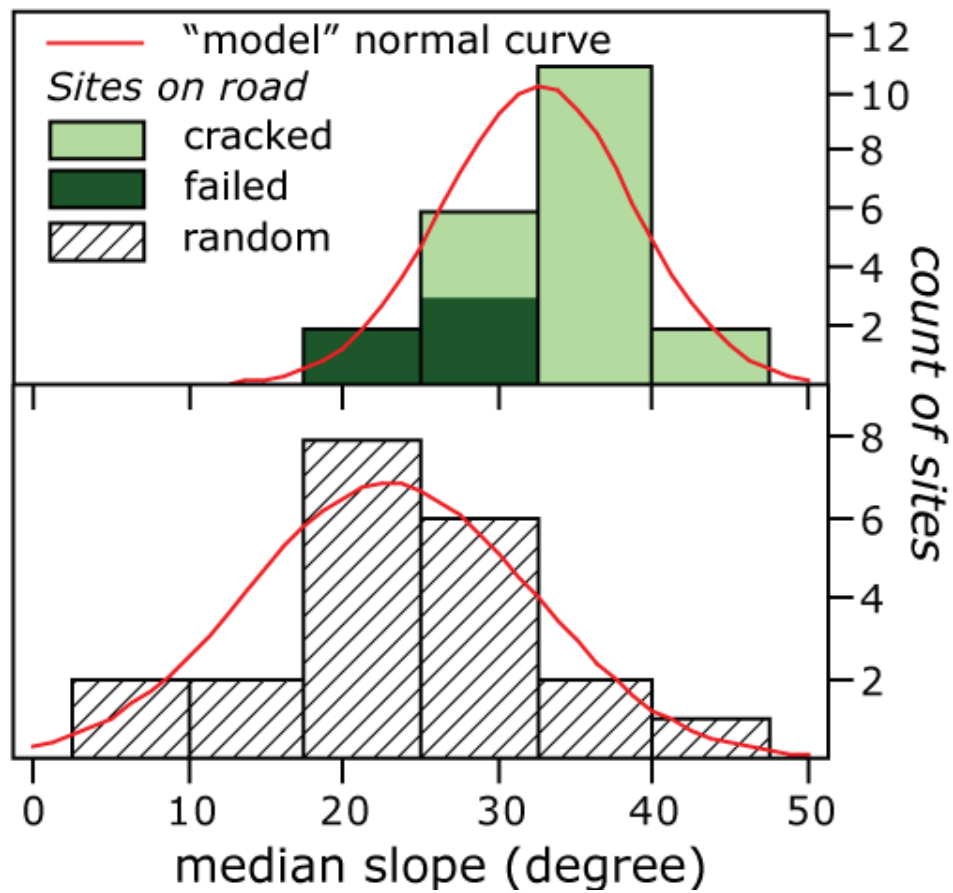


Figure 20. Frequency distributions of individual slopes.

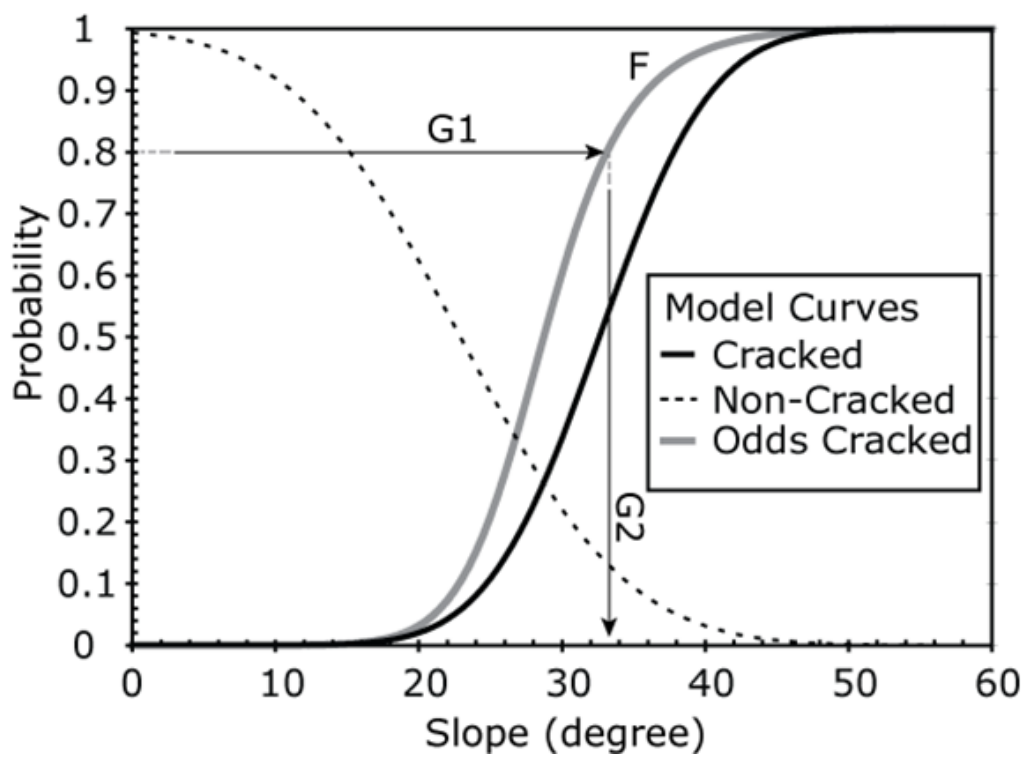


Figure 21. Probabilistic decision-making model.

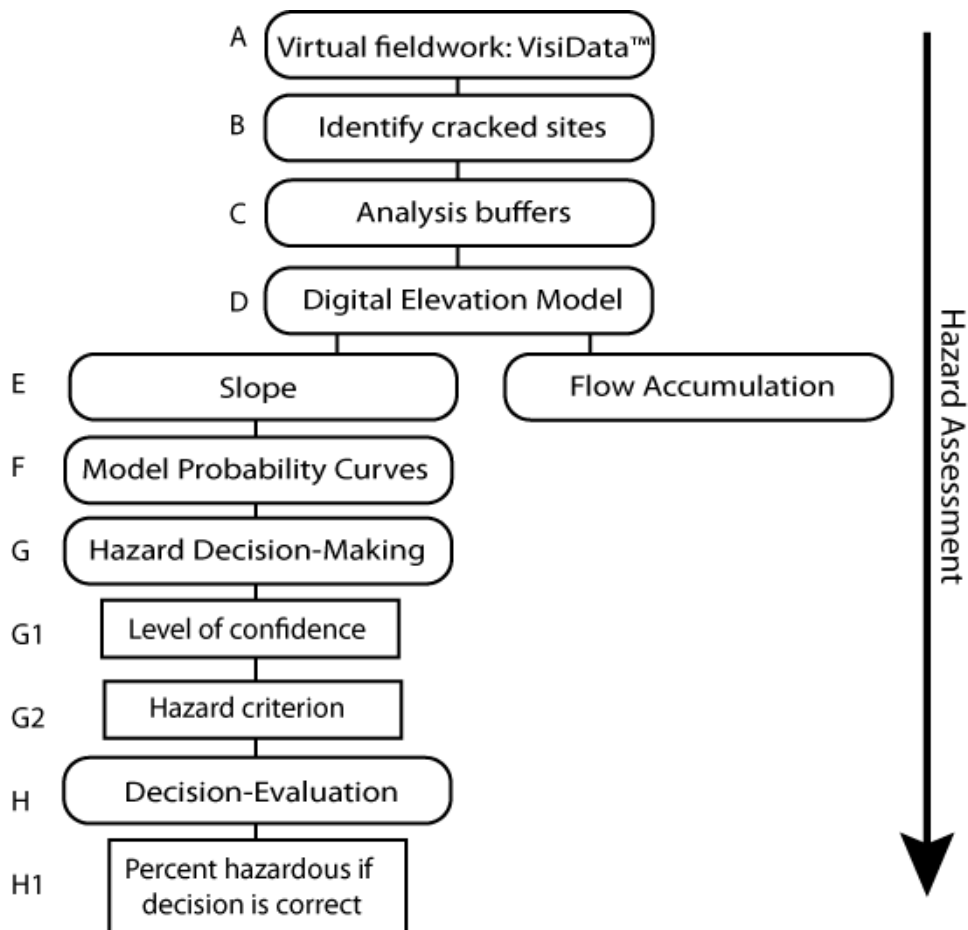


Figure 22. Flow chart of hazard assessment process using new methods.

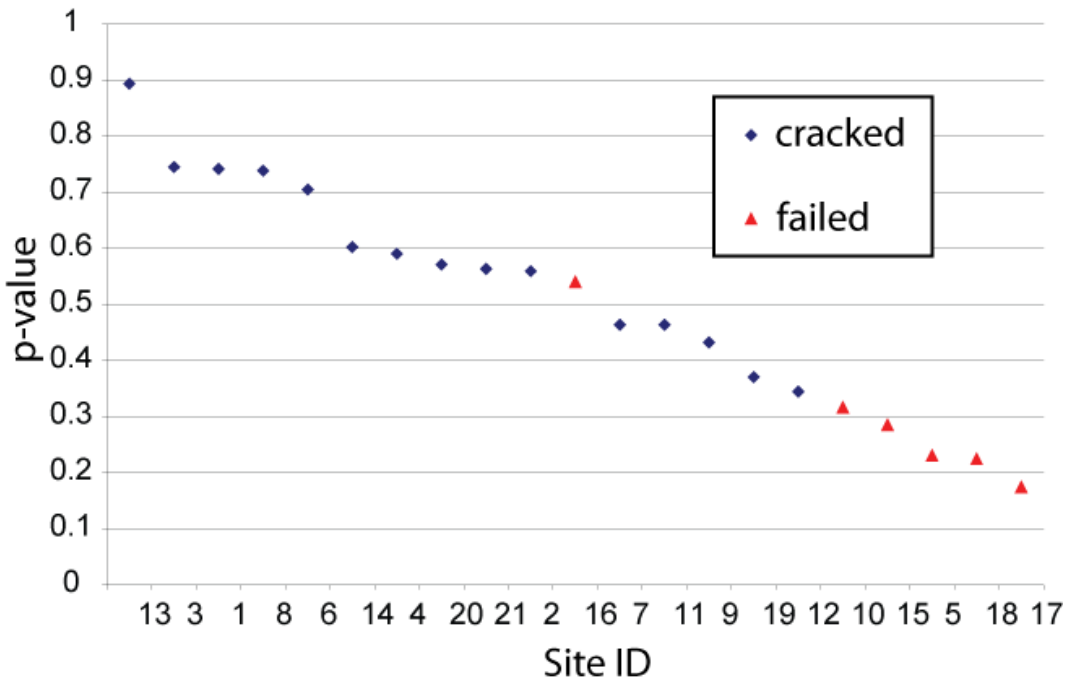


Figure 23. Under a false assumption, p-values were initially used to separate cracked and failed sites.

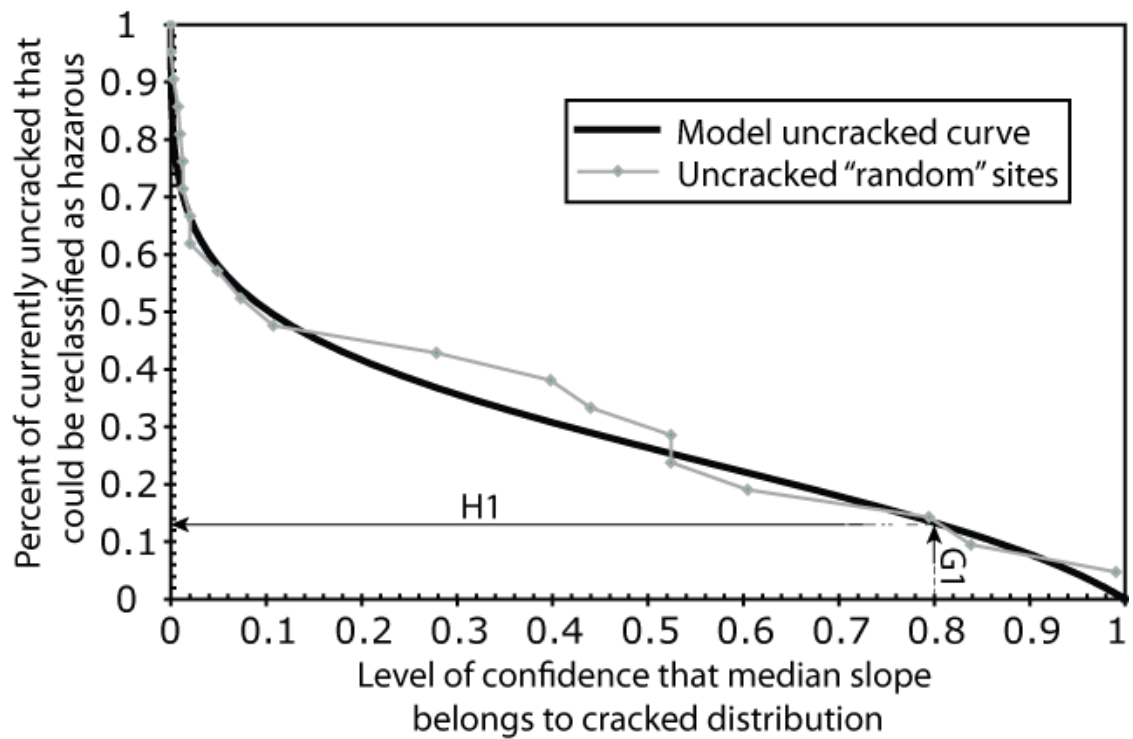


Figure 24. Decision evaluation model.

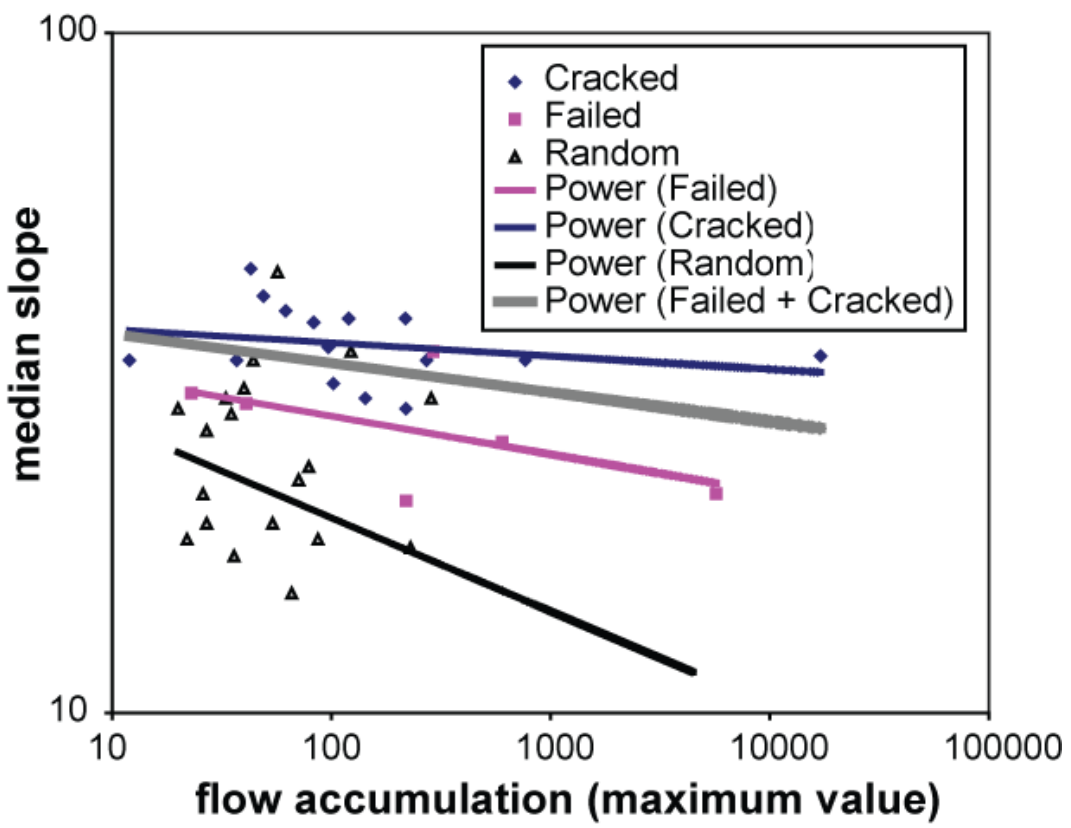


Figure 25. Plot of median slope vs. flow accumulation.

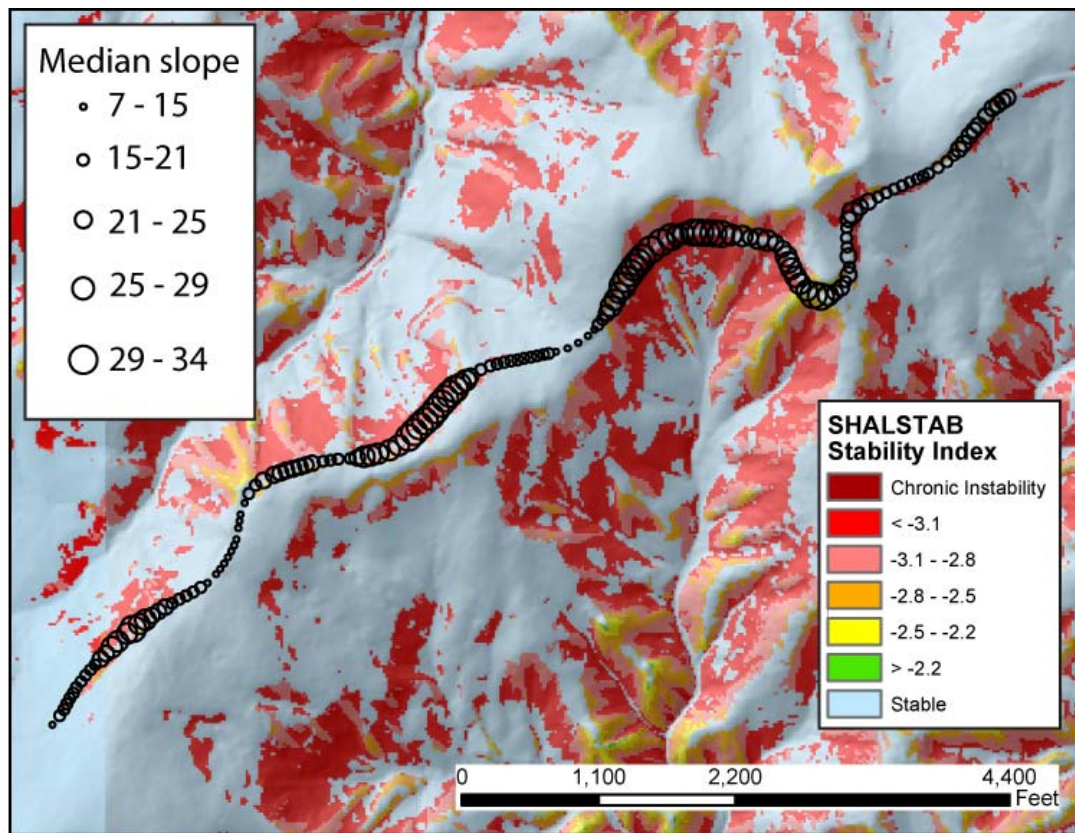


Figure 26. Map comparing median slope GIS model output to SHALSTAB model.

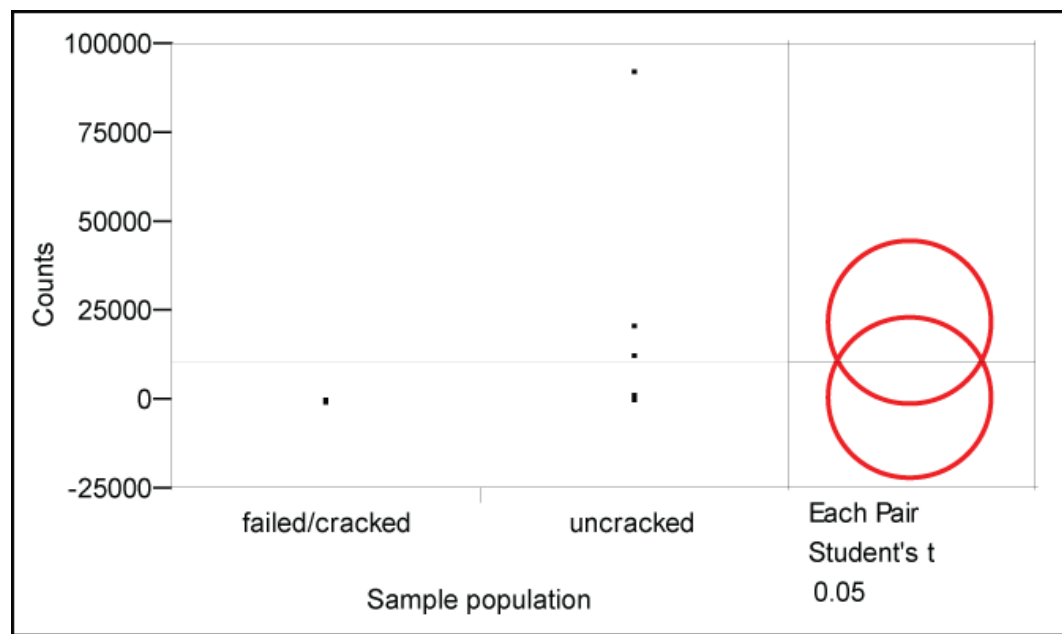


Figure 27. Student's t-test of SHALSTAB results.

Slope Distribution	Mean	Median	st. dev.	n (sites)	n (cells)	std. error	std. error of difference
uncracked, lumped	21.9	22	11.12	–	126,035	0.03	0.29
failed-cracked, lumped	31.55	33	9.86	–	1,166	0.33	0.29
<hr/>							
uncracked-random, site medians	22.93	22	9.2	21	56 per site	2.01	2.42
failed-cracked, site medians	32.6	33	6.16	21	56 per site	1.34	2.42

Table 1. Statistics from t-test for slope distributions.

9 Appendix I: Index of Field Photos by Failed-or-Cracked Site



Site 1



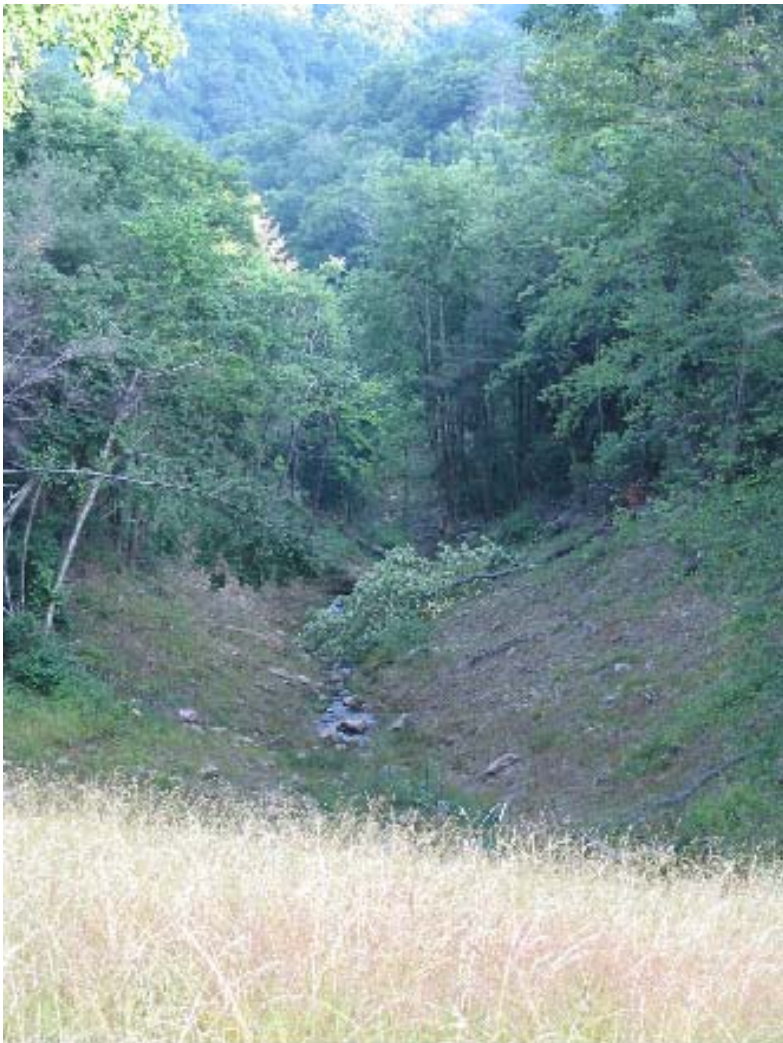
Site 2



Site 3



Site 4



Site 5



Site 6



Site 7



Site 8



Site 9



Site 10



Site 11



Site 12



Site 13



Site 14 – Arcuate form pavement crack shows lateral and vertical displacement.



Site 15 – Pavement cracks are sign of reactivation of repaired fill-slope in 2004. Wall-displacement occurred during original failure.



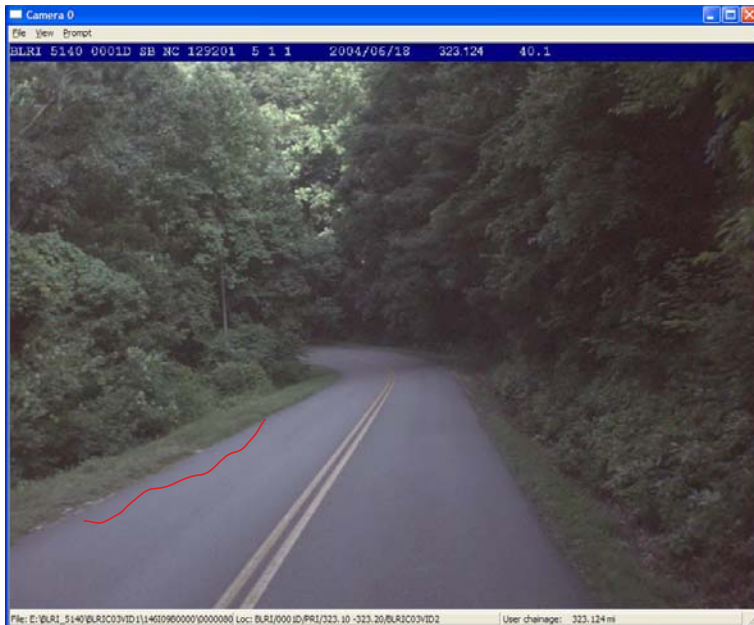
Site 16



Site 17 – Failure repair previous to September 2004



Site 18 – Rock gabion used to mitigate failure at MP 348.8



Site 19 – No field photo available; crack is visible, but faint in VisiData



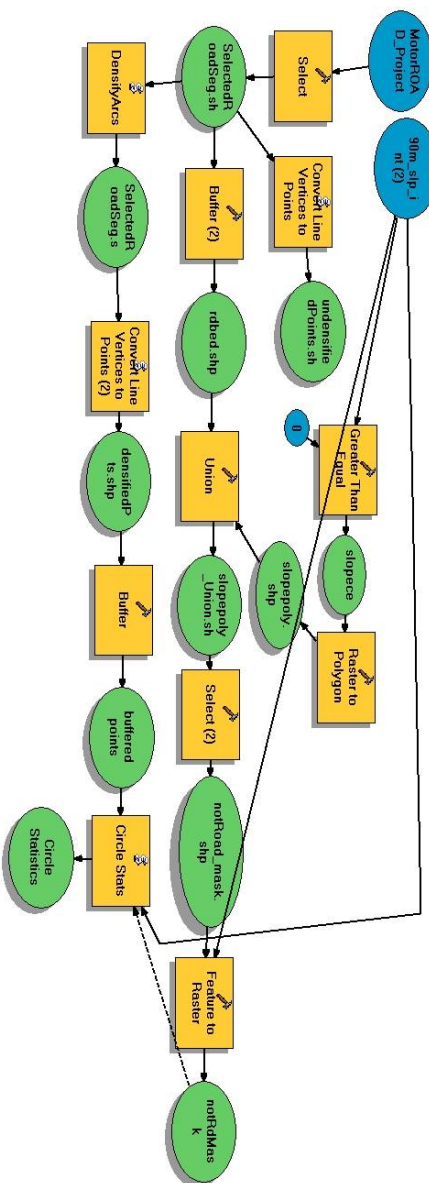
Site 20



Site 21

10 Appendix II: Modelbuilder diagram and Python scripts

Modelbuilder diagram



Compiled GIS Analysis Script (BRPtoStats.py)

```

# -----
# BRPtoStats.py
# Created on: Mon Mar 17 2008 04:21:34 PM
# (generated by ArcGIS/ModelBuilder)
# -----


# Import system modules
import sys, string, os, arcgisscripting

# Create the Geoprocessor object
gp = arcgisscripting.create()

# Check out any necessary licenses
gp.CheckOutExtension("spatial")

# Load required toolboxes...
gp.AddToolbox("C:/Program Files/ArcGIS/ArcToolbox/Toolboxes/Spatial Analyst Tools.tbx")
gp.AddToolbox("C:/Program Files/ArcGIS/ArcToolbox/Toolboxes/Conversion Tools.tbx")
gp.AddToolbox("C:/docs/py/geomorph/BRPtools.tbx")
gp.AddToolbox("C:/Program Files/ArcGIS/ArcToolbox/Toolboxes/Analysis Tools.tbx")


# Local variables...
SelectedRoadSeg_shp = "C:\\docs\\py\\geomorph\\SelectedRoadSeg.shp"
buffered_points = "C:\\docs\\py\\geomorph\\densifiedRdPts_Buffer.shp"
rdbed_shp = "C:\\docs\\py\\geomorph\\rdbed.shp"
slopecells = "C:\\docs\\py\\geomorph\\slopecells"
v0 = "0"
slopepoly_shp = "C:\\docs\\py\\geomorph\\slopepoly.shp"
slopepoly_Union_shp = "C:\\docs\\py\\geomorph\\slopepoly_Union.shp"
notRoad_mask_shp = "C:\\docs\\py\\geomorph\\notRoad_mask.shp"
undensifiedPoints_shp = "C:\\docs\\py\\geomorph\\undensifiedPoints.shp"
SelectedRoadSeg_shp_2 = "C:\\docs\\py\\geomorph\\SelectedRoadSeg.shp"
Circle_Statistics = "C:\\docs\\py\\geomorph\\zonalStats.dbf"
densifiedPts_shp = "C:\\docs\\py\\geomorph\\densifiedPts.shp"

```

```

v90m_slp_int_2_ = "C:\\docs\\py\\geomorph\\90m_slp_int"
MotorROAD_Project1_shp_2_ = "C:\\docs\\py\\geomorph\\MotorROAD_Project1.shp"
notRdMask = "C:\\docs\\py\\geomorph\\notRdMask"

# Process: Select...
gp.Select_analysis(MotorROAD_Project1_shp_2_, SelectedRoadSeg_shp, "\"FID\" = 15")

# Process: Convert Line Vertices to Points...
gp.toolbox = "C:/docs/py/geomorph/BRPtools.tbx"
gp.lines2pts(SelectedRoadSeg_shp, undensifiedPoints_shp)

# Process: DensifyArcs...
gp.toolbox = "C:/docs/py/geomorph/BRPtools.tbx"
gp.DensifyArcs(SelectedRoadSeg_shp, "100", "0")

# Process: Convert Line Vertices to Points (2)...
gp.toolbox = "C:/docs/py/geomorph/BRPtools.tbx"
gp.lines2pts(SelectedRoadSeg_shp_2_, densifiedPts_shp)

# Process: Buffer...
gp.Buffer_analysis(densifiedPts_shp, buffered_points, "100 Feet", "FULL", "ROUND", "NONE", "")

# Process: Greater Than Equal...
gp.GreaterThanEqual_sa(v90m_slp_int_2_, v0, slopecells)

# Process: Raster to Polygon...
gp.RasterToPolygon_conversion(slopecells, slopepoly_shp, "NO_SIMPLIFY", "VALUE")

# Process: Buffer (2)...
gp.Buffer_analysis(SelectedRoadSeg_shp, rdbed_shp, "10 Feet", "FULL", "ROUND", "ALL", "")

# Process: Union...
gp.Union_analysis("C:\\docs\\py\\geomorph\\slopepoly.shp #", slopepoly_Union_shp, "ALL", "", "GAPS")

```

```

# Process: Select (2)...
gp.Select_analysis(slopepoly_Union_shp, notRoad_mask_shp, "\"FID_rdbed\" = -1")

# Process: Feature to Raster...
tempEnvironment0 = gp.XYResolution
gp.XYResolution = ""
tempEnvironment1 = gp.scratchWorkspace
gp.scratchWorkspace = ""
tempEnvironment2 = gp.MTolerance
gp.MTolerance = ""
tempEnvironment3 = gp.randomGenerator
gp.randomGenerator = "0 ACM599"
tempEnvironment4 = gp.outputCoordinateSystem
gp.outputCoordinateSystem = ""
tempEnvironment5 = gp.outputZFlag
gp.outputZFlag = "Same As Input"
tempEnvironment6 = gp.qualifiedFieldNames
gp.qualifiedFieldNames = "true"
tempEnvironment7 = gp.extent
gp.extent = "C:\\docs\\py\\geomorph\\90m_slp_int"
tempEnvironment8 = gp.XYTolerance
gp.XYTolerance = ""
tempEnvironment9 = gp.cellSize
gp.cellSize = "20"
tempEnvironment10 = gp.outputZValue
gp.outputZValue = ""
tempEnvironment11 = gp.outputMFlag
gp.outputMFlag = "Same As Input"
tempEnvironment12 = gp.geographicTransformations
gp.geographicTransformations = ""
tempEnvironment13 = gp.ZResolution
gp.ZResolution = ""
tempEnvironment14 = gp.workspace
gp.workspace = ""
tempEnvironment15 = gp.MResolution
gp.MResolution = ""
tempEnvironment16 = gp.ZTolerance
gp.ZTolerance = ""

```

```

gp.FeatureToRaster_conversion(notRoad_mask_shp, "FID_slopep", notRdMask,
v90m_slp_int_2_)
gp.XYResolution = tempEnvironment0
gp.scratchWorkspace = tempEnvironment1
gp.MTolerance = tempEnvironment2
gp.randomGenerator = tempEnvironment3
gp.outputCoordinateSystem = tempEnvironment4
gp.outputZFlag = tempEnvironment5
gp.qualifiedFieldNames = tempEnvironment6
gp.extent = tempEnvironment7
gp.XYTolerance = tempEnvironment8
gp.cellSize = tempEnvironment9
gp.outputZValue = tempEnvironment10
gp.outputMFlag = tempEnvironment11
gp.geographicTransformations = tempEnvironment12
gp.ZResolution = tempEnvironment13
gp.workspace = tempEnvironment14
gp.MResolution = tempEnvironment15
gp.ZTolerance = tempEnvironment16

# Process: Circle Stats...
tempEnvironment0 = gp.cellSize
gp.cellSize = "MAXOF"
tempEnvironment1 = gp.mask
gp.mask = "C:\\docs\\py\\geomorph\\notRdMask"
gp.toolbox = "C:/docs/py/geomorph/BRPtools.tbx"
gp.circlestats(buffered_points, v90m_slp_int_2_, Circle_Statistics)
gp.cellSize = tempEnvironment0
gp.mask = tempEnvironment1

```

Densify Arcs (*DensifyArcs.py*)

```

# -----
# DensifyArcs.py
# Created Mar 2008
# Jerry Davis and Barry Nickel
# Institute for Geographic Information Science
# San Francisco State University

```

```

# -----
# Import system modules
import sys, string, os, arcgisscripting

# Create the Geoprocessor object
gp = arcgisscripting.create()

# Load required toolboxes...
gp.AddToolbox("C:/Program Files/ArcGIS/ArcToolbox/Toolboxes/Data Management Tools.tbx")

inputLines = sys.argv[1]
distance = sys.argv[2]
tolerance2 = sys.argv[3]
gp.SetParameterAsText(3, inputLines)

# Local variables...
roadsegment_2_ = "roadsegment"
roadsegment = "roadsegment"

# Process: Calculate Field...
VBAstart = "Dim pGeometry As IGeometry\\nDim pPolycurve As IPolycurve\\nDim dTol1 As Double\\nDim dTol2 As Double\\nDim pTopOp As ITopologicalOperator\\n\\ndTol1 = "
VBAmid = "\\ndTol2 = "
VBAend = "\\n\\nIf (Not IsNull([Shape])) Then\\n  Set pGeometry = [Shape]\\n  If (Not pGeometry.IsEmpty) Then\\n    If (pGeometry.GeometryType = esriGeometryPolygon) Or (pGeometry.GeometryType = esriGeometryPolyline) Then\\n      Set pPolycurve = pGeometry\\n      pPolycurve.Densify dTol1, dTol2\\n    End If\\n  End If\\nEnd If"
VBAstring = VBAstart + distance + VBAmid + tolerance2 + VBAend

gp.CalculateField_management(inputLines, "Shape", "pGeometry", "VB", VBAstring)

```

Convert Line Vertices to Points (*lines2pts.py*)

```

# -----
# Convert Line Vertices to Points

```

```

# Created Mar 2008
# Jerry Davis and Barry Nickel
# Institute for Geographic Information Science
# San Francisco State University
# -----
#
import arcgisscripting, sys, os, math
gp = arcgisscripting.create()

try:
    gp.overwriteoutput = 1
    inputLines = sys.argv[1]
    outputPts = sys.argv[2]
    sPath, sName = os.path.split(outputPts)
    if gp.exists(outputPts):
        gp.delete_management(outputPts)
    sr = gp.CreateSpatialReference("#", str(inputLines))
    gp.CreateFeatureClass_management(sPath, sName, "point", "#", "#", "#", sr)
    # Set up input lines
    lines = gp.SearchCursor(inputLines)
    points = gp.InsertCursor(outputPts)
    line = lines.Next()
    while line:
        linefeat = line.shape
        a = 0
        while a < linefeat.PartCount:
            # Process vertices into points for this line
            lineArray = linefeat.GetPart(a)
            lineArray.Reset
            vertex = lineArray.Next()
            while vertex:
                pointfeat = points.NewRow()
                point = gp.CreateObject("Point")
                point.x = vertex.x
                point.y = vertex.y
                pointfeat.shape = point
                pointfeat.Id = a
                points.InsertRow(pointfeat)
                vertex = lineArray.Next()
                a = a + 1
            a = a + 1
        line = lines.Next()
    lines.Close()
    points.Close()

```

```

a = a + 1
line = lines.Next()
del lines
del points
gp.CalculateField(outputPts, "id", "[FID] + 1")
except:
    del lines
    del points
    msg = gp.getmessages()
    gp.addmessage(msg)
    print msg

```

Circle Statistics (circlestats.py)

```

# -----
# CircleStats.py
# Created Mar 2008
# Jerry Davis and Barry Nickel
# Institute for Geographic Information Science
# San Francisco State University
# -----
import arcgisscripting, sys, os, math
gp = arcgisscripting.create()
def sendmsg(msg):
    print msg
    gp.addmessage(msg)

try:
    gp.overwriteoutput = 1
    inputBufs = sys.argv[1]
    inputRas = sys.argv[2]
    gp.CheckOutExtension("Spatial")
    inputDesc = gp.describe(inputBufs)
    wholePath = inputDesc.CatalogPath
    sPath, sName = os.path.split(wholePath)
    tablePath1 = sPath + "/zonalStats1.dbf"
    tablePath = sPath + "/zonalStats.dbf"

```

```
tableTemp = sPath + "/temp.dbf"
gp.setparameterastext(2, tablePath)
nBufs = gp.GetCount_Management(inputBufs)
for i in range(nBufs):
    id = i+1
    selstr = ' "id" = ' + str(id)
    sendmsg(selstr)
    bufout = sPath + "/buf.shp"
    gp.select_analysis(inputBufs, bufout, selstr)
    gp.ZonalStatisticsAsTable_sa(bufout, "id", inputRas, tablePath1, "DATA")
    if id == 1:
        gp.copy_management(tablePath1, tablePath)
    else:
        gp.copy_management(tablePath, tableTemp)
        vt = gp.createobject("ValueTable")
        vt.AddRow(tableTemp)
        vt.AddRow(tablePath1)
        gp.merge_management(vt, tablePath)
except:
    msg = gp.getmessages()
    gp.addmessage(msg)
    print msg
```

GIS Model Output Attribute Table: Statistical Moments and Feature Attributes

VA LU E	C O U NT	AREA	M IN	M A X	RA NG E	MEAN	STD	SUM	VA RI ET Y	MA JO RIT Y	MIN ORI TY	M E DI A N	
1	73	29200.00	0	17	17	7.17808	4.33950	524.00	17	8	9	6	
2	72	28800.00	0	17	17	7.27778	4.36597	524.00	17	8	9	7	
3	68	27200.00	0	17	17	7.77941	3.68959	529.00	17	8	0	8	
4	67	26800.00	0	16	16	8.11940	3.86535	544.00	16	9	0	8	
5	68	27200.00	2	28	26	11.13240	6.10184	757.00	24	5	2	10	
6	69	27600.00	2	34	32	13.78260	8.45083	951.00	28	5	2	12	
								1034.0					
7	70	28000.00	0	34	34	14.77140	9.07771	0	30	5	0	14	
8	70	28000.00	0	34	34	13.71430	7.65720	960.00	27	13	0	13	
9	70	28000.00	3	32	29	13.68570	6.12849	958.00	21	13	4	14	
								1145.0					
10	70	28000.00	2	37	35	16.35710	8.91553	0	28	3	2	16	
11	70	28000.00	2	37	35	21.14290	8.58451	1480.0	0	31	19	2	21
								1561.0					
12	70	28000.00	7	34	27	22.30000	7.26312	0	25	25	7	24	
13	69	27600.00	5	34	29	21.24640	8.34823	1466.0	0	29	26	6	23
14	69	27600.00	5	35	30	22.11590	8.63350	1526.0	0	24	24	7	24
15	70	28000.00	4	35	31	20.74290	8.39504	1452.0	0	27	24	4	23
16	70	28000.00	4	35	31	17.51430	7.78413	1226.0	0	29	15	6	16
17	69	27600.00	2	34	32	16.71010	7.67851	1153.0	0	28	14	2	15
								1017.0					
18	66	26400.00	2	34	32	15.40910	7.20475	0	27	18	2	15	
19	66	26400.00	2	31	29	12.80300	5.58738	845.00	22	14	2	12	
20	67	26800.00	0	19	19	10.44780	4.78893	700.00	20	10	0	11	
21	69	27600.00	0	19	19	8.91304	4.82067	615.00	19	6	0	9	
22	70	28000.00	0	17	17	7.91429	4.24851	554.00	18	6	0	7	
23	71	28400.00	3	17	14	8.49296	3.75246	603.00	14	5	3	7	
24	71	28400.00	3	17	14	9.16901	3.87111	651.00	15	5	17	9	
25	70	28000.00	2	32	30	12.70000	6.36811	889.00	22	13	2	12	
26	70	28000.00	2	33	31	15.52860	8.80701	1087.0	29	13	2	13	

								0				
27	70	28000.00	2	33	31	15.62860	8.71972	1094.00	28	12	2	12
28	72	28800.00	4	33	29	14.75000	6.87336	1062.00	25	12	4	12
29	71	28400.00	4	25	21	14.57750	5.25052	1035.00	20	11	4	14
30	71	28400.00	0	28	28	12.21130	7.25378	867.00	27	18	1	13
31	71	28400.00	0	28	28	10.02820	7.69666	712.00	25	1	7	10
32	70	28000.00	0	24	24	9.51429	6.42482	666.00	22	8	0	8
33	70	28000.00	1	24	23	10.40000	6.20230	728.00	20	2	4	11
34	70	28000.00	0	27	27	11.48570	6.53287	804.00	25	12	0	12
35	70	28000.00	0	28	28	12.48570	8.11831	874.00	27	12	0	12
36	70	28000.00	1	29	28	13.07140	9.65449	915.00	24	3	7	12
37	69	27600.00	1	29	28	13.56520	9.47075	936.00	27	3	7	12
38	69	27600.00	2	29	27	14.21740	7.73261	981.00	26	12	6	14
39	67	26800.00	1	22	21	10.98510	6.09990	736.00	22	4	3	10
40	66	26400.00	2	21	19	10.72730	5.19774	708.00	18	7	3	10
41	65	26000.00	1	17	16	8.36923	3.63559	544.00	15	12	15	8
42	65	26000.00	1	17	16	7.55385	3.53458	491.00	15	6	3	7
43	67	26800.00	1	14	13	7.10448	2.75970	476.00	12	6	11	7
44	69	27600.00	1	13	12	6.91304	2.50066	477.00	13	6	2	7
45	70	28000.00	2	13	11	6.20000	2.62189	434.00	12	4	13	6
46	69	27600.00	2	14	12	5.95652	3.11813	411.00	13	4	2	5
47	69	27600.00	1	15	14	6.65217	3.55832	459.00	14	4	1	5
48	71	28400.00	3	17	14	8.32394	3.59097	591.00	15	6	12	8
49	70	28000.00	4	17	13	9.57143	3.63149	670.00	14	7	16	9
50	70	28000.00	2	16	14	8.74286	3.25877	612.00	15	7	2	8
51	70	28000.00	1	17	16	8.32857	3.20143	583.00	16	9	1	8
52	70	28000.00	1	21	20	9.67143	4.62515	677.00	18	4	3	9
53	69	27600.00	1	21	20	10.30430	4.83737	711.00	19	10	2	10
54	69	27600.00	2	21	19	10.34780	4.76347	714.00	18	10	5	10
55	68	27200.00	2	18	16	8.55882	3.83246	582.00	16	8	13	8
56	70	28000.00	2	17	15	7.35714	3.18943	515.00	15	7	3	7
57	69	27600.00	1	14	13	6.66667	2.45933	460.00	12	7	1	7
58	70	28000.00	0	14	14	6.14286	2.48588	430.00	13	7	0	6
59	70	28000.00	0	19	19	7.07143	3.98326	495.00	19	6	0	6
60	70	28000.00	0	20	20	9.10000	5.07979	637.00	21	5	0	8
61	69	27600.00	1	22	21	11.26090	6.01364	777.00	22	7	2	11
62	69	27600.00	1	22	21	14.42030	5.44114	995.00	21	20	1	15
63	70	28000.00	4	22	18	14.55710	4.48373	1019.0	18	16	4	15

								0					
64	71	28400.00	4	26	22	15.05630	4.72001	1069.0 0	20	15	4	15	
65	75	30000.00	2	26	24	14.14670	5.48864	1061.0 0	22	15	2	15	

11 Appendix III: Example of hazard evaluation exercise

Using the Blue Ridge Parkway Landslide Hazard Project GIS

1. Click Start > Programs > ArcGIS > ArcMap
 - 1.1. Browse for “Blue Ridge ParkwayLHP_MAP_v4” (or select the lastest version [e.g. v5, v6])
 - 1.2. Give the map time to load, it make take up to 10 minutes depending on processor speed.
2. Layers (layer names are in quotations)
 - 2.1. Hazards/Road Closure Data
 - 2.1.1. “Process_GPS” contains data collected by the NCGS for multiple types of hazards that have or have potential to occur along the Blue Ridge Parkway. Such processes include debris flow, debris slide, rock fall, road slump, etc.
 - 2.1.2. “Crack Severity” contains field data collected during the August 2006 field work for Blue Ridge ParkwayLHP Phase I. This data relates to the severity of cracks observed in the field (High, Moderate, Low) and each point is hyperlinked to a photograph of the crack(s).

2.1.3. “Road Closure Point” contains points that have historically been access points and may be used as locations to close susceptible portions of the road and for rerouting of detours. This data has not been field checked.

2.1.4. “2004sept_Blue Ridge Parkway_fillfailure_debrisflow_tracks” contains data provided by USFS that shows three failure tracks that occurred in 2004 due to fill slope failures.

2.1.5. “Parkway Failure Potential” shows the portions of the roadway that are susceptible (High, Moderate, Low) to failure based on crack severity within each mile segment of the Blue Ridge Parkway.

2.1.6. “Possible Failure Track” contains polylines that delineate the “possible” failure tracks of debris flows that may result from road fill failures.

Important Note: These possible failure tracks were delineated based only upon locations of streams, incised valleys, and “steep” slopes observed on topographic maps and aerial photos. These tracks have not been modeled or field checked, and are based solely on qualitative assessment.

2.2. Roadway Data

2.2.1. “MilepostNAD83_Project1” contains data for mileposts at one-mile intervals. These coincide with VisiData and have not been field checked.

- 2.2.2. “milepose_10” contains data for mileposts at ten-mile intervals within the study area from mile 310 to 370.
- 2.2.3. “Parkway (not studied)” contains data from VisiData that delineates the entire Blue Ridge Parkway, and thus contains data that is outside the study area of the Blue Ridge ParkwayLHP Phase I.
- 2.2.4. “NC_HWY_80” contains data delineating the location of a portion of NC State Hwy. 80. This layer is provided as a location marker that people familiar with the region may recognize.
- 2.2.5. “Calibrated_Routes” contains data similar to “Parkway (not studied)” (2.1.3.) but was calibrated differently and thus these layers do align perfectly. The accuracy of this layer requires field checking.
- 2.2.6. “Intersection_Left” contains data for the point locations (from VisiData) of roadways connecting to the Blue Ridge Parkway to the East.
- 2.2.7. “Intersection_Right” contains data for the point locations (from VisiData) of roadways connecting to the Blue Ridge Parkway to the West.
- 2.2.8. “Overlooks” contains data for the locations (from VisiData) of overlooks or pull-off locations to the East and West of the Blue Ridge Parkway.

2.3. Base Maps

2.3.1. “HillSha_ned_3” is a DEM (90-meter resolution). This DEM acts as a hillshade model processed to mimic topography.

2.3.2. “Asheville.tif” (and all other <place name>.tif) layers are USGS 7.5 Minute Quadrangle topographic maps.

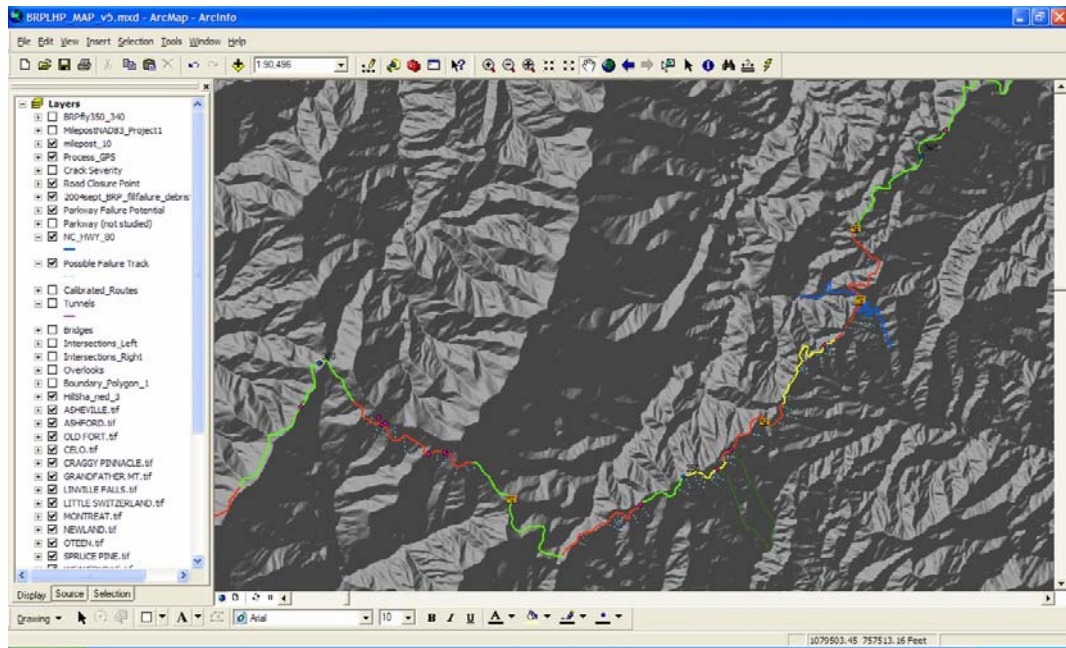
2.3.3. “ColorIRTile72.sid” (and all other ColorIRTile<number>.sid) layers are infrared digital ortho quad aerial photographs.

2.3.4. “Boundary_Polygon_1” contains data showing the boundary of the National Park Service managed lands.

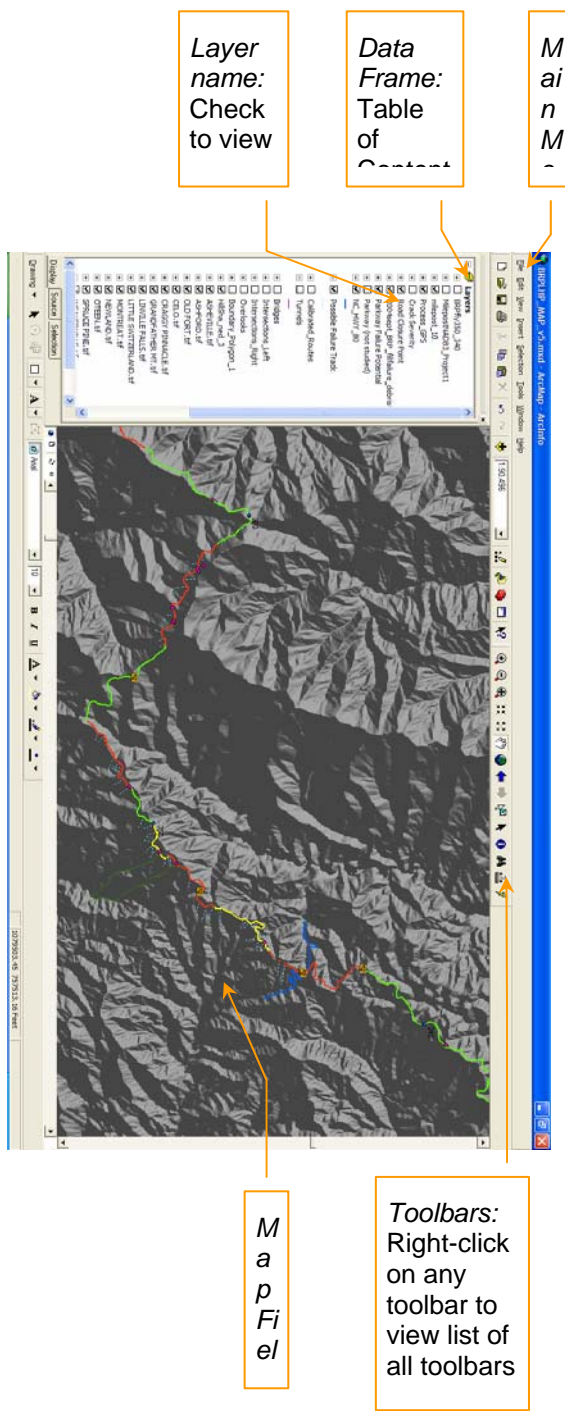
2.3.5. “states_VA_NC” is a polygon basemap for Virginia and North Carolina.

3. Using ArcMap

3.1. A typical view of the Blue Ridge ParkwayLHP-GIS may look like this:



3.2. Below is a diagram showing the essential elements of the ArcMap module:



3.3. Basic tools

3.3.1. *ArcCatalog*: Opens the file management module for ArcGIS

3.3.2. *ArcToolbox*: Analysis tools for advanced users.

3.3.3. *Zoom*: Change the scale and location of the map field.

3.3.4. *Full Extent*: Allows you to view full extent of data in map field.

3.3.5. *Hand*: Move the location of the map field.

3.3.6. *Previous/Forward View*: Go to most recent views of map field.

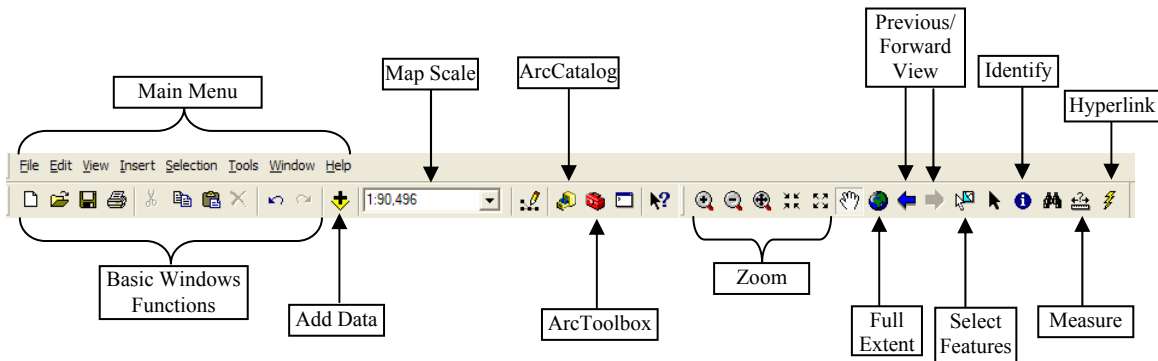
3.3.7. *Select features*: Select features on map, Ctrl-click for multiple selections.

3.3.8. *Find*: Can help locate features (does not always work well).

3.3.9. *Identify*: Use to view attributes of selectable features.

3.3.10. *Measure*: Use to make line-distance measurements (units depend on that of layer projection) displayed at bottom of ArcMap module screen.

3.3.11. *Hyperlink (lightening bolt)*: Use to open hyperlinked photos or documents.



3.4. Viewing and Navigating Data Layers

3.4.1. To make layers viewable in the map field be sure the layer is “checked” in the Table of Contents.

3.4.2. The first layer in the Table of Contents will be the top most viewable layer. Layers may need to be moved to increase visibility.

3.5. Assessing Weather System

3.5.1. If shapefile of precipitation is available import into ArcMap using the *Add Data* button

3.5.2. If weather system is large, then consider the basins which demonstrate the most potential for failure. Criteria that increase susceptibility include:

3.5.2.1. Drainage basins that face the storm front.

3.5.2.2. Higher elevations.

3.5.2.3. Regional swales in mountain range topography that would act to “trap” weather system.

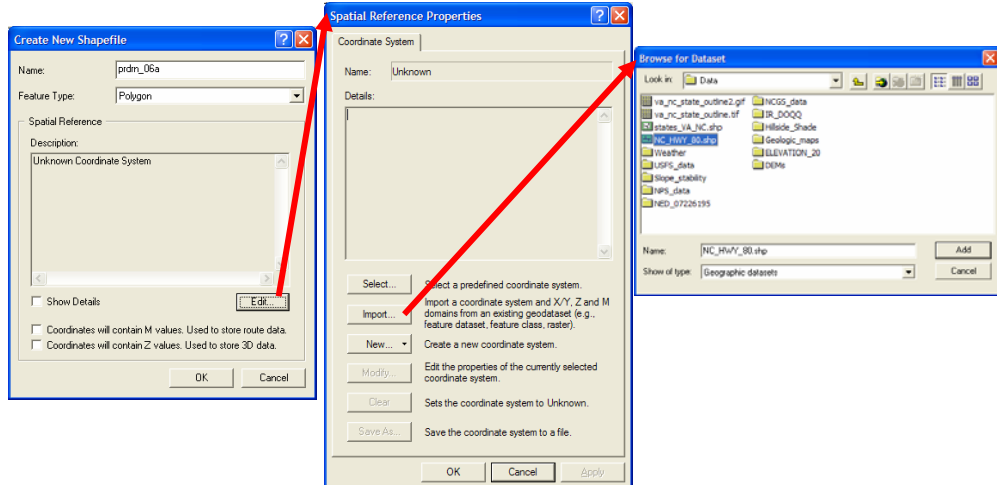
3.5.2.4. Areas known to commonly have higher levels of precipitation during rain events.

3.6. Creating a Record of the Predicted Rainfall

3.6.1. Once the areas predicted to receive heavy rainfall are known create a new shapefile and digitize these basins.

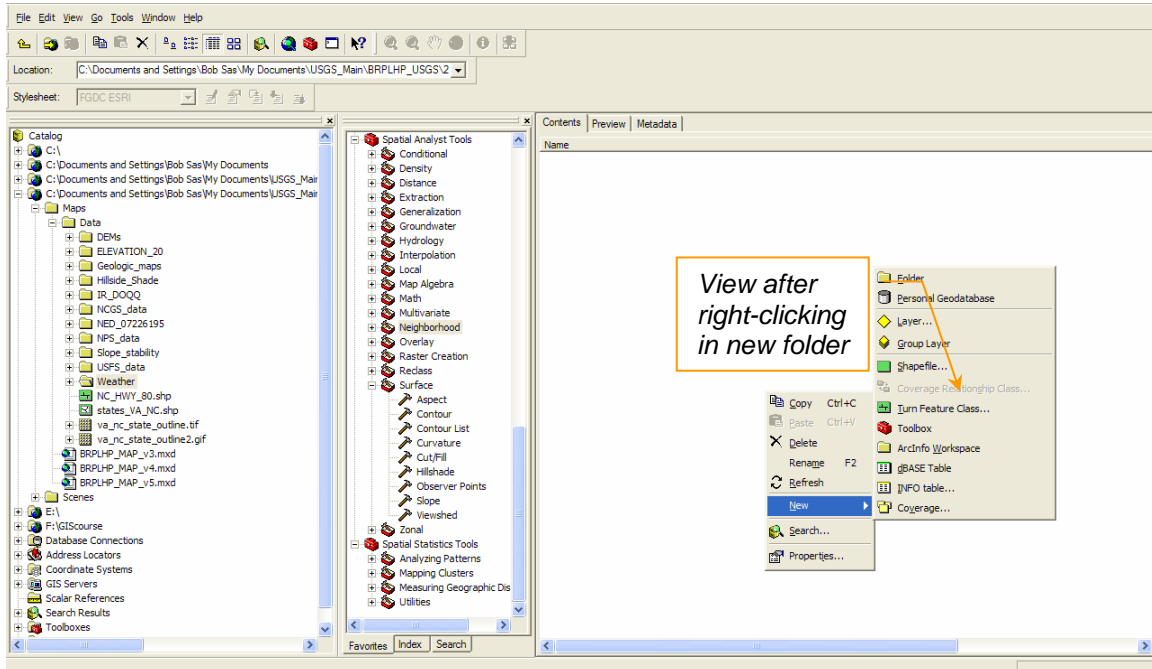
3.6.2. Open ArcCatalog by clicking on the button on the toolbar or by Start > Programs > ArcGIS > ArcCatalog

3.6.3. Navigate to the folder to save the shapefile in or create a new folder by



right-clicking on an existing folder > New > Folder.

3.6.4. Right-click in the new folder > New > Shapefile



3.6.5. Name the shapefile “prdrn_06a”; this nomenclature means: “prdrn” = predicted rainfall; “06” = year 2006; “a” = the first storm of the year 2006

3.6.6. Feature Type select: Polygon

3.6.7. To define the coordinate system click the “Edit” button > Import. Navigate to a folder containing Blue Ridge ParkwayLHP-GIS datasets and select a shapefile. (This will make the coordinate system of the new shapefile match that of an existing shapefile.)

3.6.8. Click Add > OK > OK

3.6.9. Once you've added the new shapefile you can begin digitizing on the layer.

3.6.10. In the Main Menu click View > Toolbars > Editor

3.6.11. In the Editor toolbar click Start Editing. In the pop-up menu be sure to select the file set that contains the prdrn_06a shapefile.

3.6.12. In the Editor toolbar make sure that:

3.6.12.1. Task: Create New Feature is selected

3.6.12.2. Target: prdrn_06a is selected

3.6.13. Begin digitizing the polygon of where heavy rain is predicted to fall by



clicking the Pencil tool in the Editor toolbar.

3.6.14. To digitize the polygon left-click on the map field and continue to click points to create line segments. To close the polygon double-click on the starting point.

3.6.15. You can create as many new polygons as necessary on this layer.

3.6.16. When you are finished digitizing click Editor > Save Edits > Stop Editing.

3.7. Performing a Spatial Selection Query

3.7.1. Although there are several methods that can help highlight the areas that will receive heavy rainfall I will use the simplest

3.7.2. In the main menu click Selection > Select by Location

3.7.3. In the window that opens input:

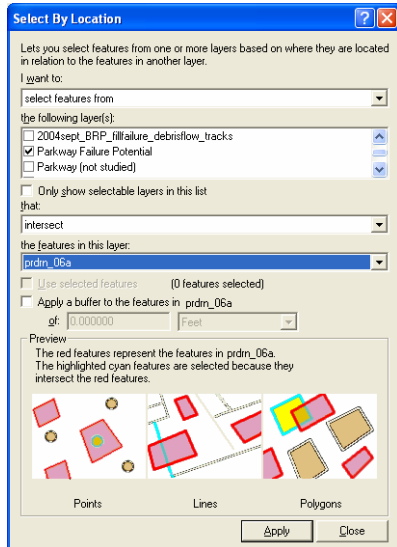
3.7.3.1. I want to: “Select features from”

3.7.3.2. the following layer: “Parkway Failure Potential”

3.7.3.3. that: “intersect”

3.7.3.4. the features in this layer: “prdrn_06a”

3.7.3.5. the screen should look like this:



3.7.3.6. Click Apply

3.7.4. Now you have selected the portions of roadway that should be considered for road closure.

3.8. Selecting Road Closure Points

3.8.1. Now that the potential failure areas are recognized, road closure can begin.

3.8.2. The layer “Road Closure Point” contains the sites that may have gates and potential detour routes.

3.8.3. Identify the road closure points (labeled with a yellow “Detour sign” symbol) within the selected region (See section 3.7), or that are near the extents of the “prdrn_06a” polygon.

3.8.4. Use chain of command to dispatch trained personnel to close portions of roadway.

12 Appendix IV: Data collected during virtual fieldwork

Mile Begin	Mile End	Crack Code	Notes	Lane Code	Loca tion Note	PC R	SC R	S e v e r i t y	LAT	LON
307.280	307.302	A	Multiple half circle patches	S		63	84		36.0 5669 8	81.8 503 42
310.674	310.820	C	Severe alligator cracking	N		100	10 0		36.0 1852 8	81.8 786 85
310.314		C L T	Intersecting set of T,L	NC		97	95		36.0 2193 8	81.8 740 01
310.202		A		N		84	10 0		36.0 2285 4	81.8 722 00
310.030		C		C		74	86		36.0 2497 1	81.8 727 57
318.060	318.080	A	Visible in Camera 4	S		86	89		35.9 5782 1	81.9 599 23
318.687		A ?	Dark area difficult to see??	N		100	10 0		35.9	81.9

									4898 6	600 52
319.480		A	Patched A crack, concave, low vegetation	N		95	95		35.9 3915 6	81.9 566 80
319.541		A	Depressed area, concave, low vegetation	N		100	10 0		35.9 3843 8	81.9 572 98
319.582		T	Diagonal across both lanes	NS		100	10 0		35.9 3790 8	81.9 575 81
319.609		T		NS		100	10 0		35.9 3668 7	81.9 584 96
319.669		T L	May develop into A	N		100	10 0		35.9 3651 2	81.9 587 86
319.712	319.724	A	Depressed area, concave, low vegetation	N	Ends at MP 320	100	10 0		35.9 3635 6	81.9 590 84
319.896		L	Tension cracks due to movement?	S		97	10 0		35.9 3450 9	81.9 587 25
319.936	320.000	A	Depressed area, concave, low vegetation	S		78	88 5		35.9 3406 7	81.9 582 60
320.320	320.445	L	L and patches	S	Edge of lane	74	69		35.9 2924 1	81.9 551 09
321.639		A	Patched area	N	Edge of lane	96	93		35.9 1466 1	81.9 639 59
322.688		A s	Severe, depressed, wide cracks	N		75	87 5		35.9 0416 7	81.9 671 86

343.536		A		S		86	88		35.7 7212 9	82.1 671 30	-
343.586		A		S		98	96		35.7 7176 7	82.1 665 73	-
343.936		A		N		88	90		35.7 6751 3	82.1 664 73	-
344.066		A		N		82	84	5	35.7 6604 5	82.1 674 35	-
344.168		A		N		94	96		35.7 6474 8	82.1 681 14	-
344.832		A		N		99	99		35.7 5780 9	82.1 760 79	-
345.046		L A m	Parallel set of ~3 L cracks	S	Near road side	18	0		35.7 5587 1	82.1 782 61	-
345.824	345.842	A	Concave side slope, low vegetation	N		99	99	4	35.7 5305 2	82.1 835 56	-
345.884		T		N		85	96		35.7 5239 9	82.1 842 58	-
346.028		A	Possible depression of road	N		92	97		35.7 5045 8	82.1 848 07	-
346.288		A s		N		100	10 0	4	35.7 4718 1	82.1 869 89	-
346.414		A s		S		71	79		35.7	82.1	-

									4528 9	878 36
346.652		T L	Intersection set of T,L/Concave,low vegetation side slope	C		90	96		35.7 4254 6	- 82.1 887 82
346.748	346.782	C L	Concave side slope, low vegetation	N		96	99	4	35.7 4147 0	- 82.1 898 42
346.934	346.948	L		NS		99	99		35.7 3874 7	- 82.1 892 93
346.958		A ?	Large patched area with new tension cracks adj. to patch	S		97	95		35.7 3856 0	- 82.1 895 68
347.534		L A	Multiple	O	Pull- off	78	75		35.7 3821 3	- 82.1 973 04
348.368	348.464	A s L		N		100- 68	10 0- 68	5	35.7 2988 1	- 82.2 044 91
348.750		L		C		82	73		35.7 2620 4	- 82.2 068 86
348.788		m		S		89	93		35.7 2572 3	- 82.2 072 75
348.848		A m		N		100	10 0		35.7 2520 1	- 82.2 081 07
348.850		A		N		100	10 0		35.7 2520 1	- 82.2 081 07
349.286		A		N		95	10 0		35.7 2343	- 82.2 137

									4	15
349.446		A		N		100	10 0		35.7 2380 4	82.2 163 85
349.602		L		N		97	95		35.7 2284 7	82.2 189 48
349.607	349.632	A	Multiple	N		99	99		35.7 2284 7	82.2 189 48
349.660		A		S		97	95		35.7 2242 4	82.2 198 64
350.020		A		O	N entra nce to pull- off	99	98		35.7 1792 6	82.2 227 17
350.196		L		C		93	88 2		35.7 1798 7	82.2 255 55
350.286	350.426	T ? L		N		100	10 0		35.7 1828 1	82.2 269 06
350.626		A		S		92	96		35.7 1587 8	82.2 320 18
350.856		A L		N		96	10 0		35.7 1364 2	82.2 352 22
350.922		L		N		99	98		35.7 1324 2	82.2 361 91
351.429		L		S		96	96		35.7 1186	82.2 421

					Mile mark er				8	57
351.638		A		S	352	65	77		35.7 0966 0	- 82.2 447 66
351.854		A		S		87	93		35.7 0803 5	- 82.2 479 55
351.970	352.006	L	Multiple	S	Over look Ahea d sign	77	79		35.7 0732 9	- 82.2 494 66
352.030		L T	Intersection set of T,L	N		95	92		35.7 0713 4	- 82.2 508 62
352.096	352.108	A		S		77	65	5	35.7 0684 8	- 82.2 518 62
352.345		L		S		76	81	1	35.7 0412 4	- 82.2 541 20
352.422		L A		S		85	88		35.7 0350 6	- 82.2 553 18
352.476		A		S		54	38	5	35.7 0290 8	- 82.2 560 81
352.754		L		N	Adj. to outcr op	80	75		35.7 0105 7	- 82.2 597 73
404.640		A	Patches, multiple cracks	NS		69	89		35.4 3837 0	- 82.7 266 16
					Aver age	88.7 857	58 9			
					Medi	95	96			

Mile Begin	Mile End	C r a c k C o d e	Notes	Lane Code	Loca tion Note	PC R	SC R	S e v e r i t y	LAT	LON
---------------	-------------	---	-------	--------------	----------------------	---------	---------	--------------------------------------	-----	-----

13 Appendix V: Road Closure Protocols

- I. Evaluation of Weather System and Precipitation
 - A. Heavy rainfall warning (See also: Caveat Emptor: Antecedent Rainfall)
 - B. National Weather Service warnings, USGS Landslide Warnings, States of Emergency, Flood Warnings, or expectation of heavy rainfall should all be watched closely. Heavy rains are what ultimately result in potentially hazardous failures. Normally the most devastating rainfall occurs at a high intensity (i.e. multiple inches per hour). Rainfall can be tracked using IFLOWS via the internet <<http://www.afws.net/>> and if a deluge is expected on susceptible portions of the Blue Ridge Parkway, then the USGS Extreme Storms Team should be contacted.
 - C. Communication with USGS
 - D. Contacting the USGS extreme storms team is at the discretion of the Resource Managers, or acting Resource Managers. If the following observations are valid for the circumstance of the storm then the USGS should be contacted:
 - i. Intensity – Duration Thresholds (adapted from Madison County, VA thresholds)

- ii. See Also: Caveat Emptor: Rainfall Prediction Errors
- iii. Is rainfall is spatially distributed over susceptible portion?

<http://www.weather.gov/regsci/gis/shapefiles/>

<http://www.weather.gov/largemap.php>

<http://www.weather.gov/forecasts/graphical/sectors/conus.php?element=QPF>
- iv. Culvert is backed up and overflowing in susceptible portion

E. Road Closure Required

Intensity (in/hr)	Duration (hrs)
1 to 2	> 6
2 to 3	> 2
> 3	> 1

- i. In the event that NPS decides to close a susceptible portion of the parkway then the GIS can be used to locate the nearest road closure points.
- ii. A document must be written by resource manager to describe reasoning leading to failure including rainfall data, data's source,

and use of the GIS. This is important for evaluation and refinement of the Program.

- iii. LEOs/maintenance dispatched to close portions of roadway
- iv. Provide detour assistance to motorists

II. Brochure for the public

III. Post Warning and Detour Signs

IV. Re-Opening the Roadway

- A. Re-Opening the Roadway should only be considered once all high intensity rainfall has passed. If the ground is well-saturated a period of drying is best to be sure that the fill has time to drain and dry. Road failures are still possible after rain has passed and drying time is observed.
- B. It is best to investigate most susceptible portions prior to re-opening.
- C. The USGS can be consulted though it is not necessary.